CHARACTERIZATION OF THE NSPS-MBAA SIGNALING SYSTEM CONTROLLING BIOFILM FORMATION FROM POLYAMINE INPUT TO PHENOTYPIC OUTPUT

A Thesis
By
RICHARD CHARLES SOBE

Submitted to the Graduate School
at Appalachian State University
in partial fulfillment of the requirements for the degree of
MASTER OF SCIENCE

December 2015
Department of Biology

CHARACTERIZATION OF THE NSPS-MBAA SIGNALING SYSTEM CONTROLLING BIOFILM FORMATION FROM POLYAMINE INPUT TO PHENOTYPIC OUTPUT

A Thesis
By
RICHARD CHARLES SOBE
December 2015

APPROVED BY:

_____
Ece Karatan, PhD
Chairperson, Thesis Committee

_____
Ted Zerucha, PhD
Member, Thesis Committee

_____
Darren Seals, PhD
Member, Thesis Committee

_____
Zack E. Murrell, PhD
Chairperson, Department of Biology

_____
Max C. Poole, PhD
Dean, Cratis D. Williams School of Graduate Studies

Abstract

CHARACTERIZATION OF THE NSPS-MBAA SIGNALING SYSTEM CONTROLLING BIOFILM FORMATION FROM POLYAMINE INPUT TO PHENOTYPIC OUTPUT

Richard Charles Sobe
B.S., Appalachian State University
M.S., Appalachian State University

Chairperson: Ece Karatan

Biofilm formation is an important aspect of bacterial persistence in challenging environments. The bacterial pathogen, *Vibrio cholerae*, is an excellent biofilm former and this lifestyle has been implicated as playing a critical role in the pathogenicity of this microbe. Among the wide array of environmental signals that control *V. cholerae* biofilm formation are a select set of polyamines, norspermidine and spermidine. Norspermidine has a positive influence on biofilm formation while spermidine has the opposite effect, and these influences have been shown previously to occur through a signaling system comprised of the periplasmic binding protein, NspS, and the transmembrane phosphodiesterase, MbaA. In the absence of NspS, MbaA acts as a phosphodiesterase cleaving the pro-biofilm second messenger, cyclic di-GMP, indicating that NspS may interact with and inhibit phosphodiesterase activity and biofilm repression by MbaA. Recent work has shown that mutation of conserved amino acids in the proposed ligand-binding pocket of NspS results in drastic alterations of biofilm phenotypes. However, the exact mechanism underlying these influences remained to be elucidated and the capacity of these mutants to support polyamine

signaling had not been investigated. In this study, I have shown that several *nspS* binding pocket mutants have altered sensitivity to norspermidine and spermidine as indicated by *vps* transcription and biofilm assays. I have also shown using thermal shift assays that all of these mutants are capable of binding both polyamines. LC-MS/MS analyses indicate that the NspS-MbaA signaling pathway is a high specificity c-di-GMP signaling system. Additionally, a system for reproducible demonstration of the NspS-MbaA interaction was developed which may subsequently be used in future experiments to study the NspS and MbaA interaction and also to identify an MbaA-interaction surface on NspS. Altogether, this study provides a thorough investigation of the steps involved in polyamine signal input to phenotypic output for a novel polyamine responsive signaling system controlling biofilm formation.

Acknowledgements

I would like to recognize the Cratis D. Williams Graduate School at Appalachian State University for its assistance during my time as a graduate student. Much appreciation goes to the Graduate Student Association Senate and the Office of Student Research for funding. I am very grateful to Sue Bauldry and Audrey Brown for their assistance with generation of the NspS antibody, and to Allison Gardzalla, Jacob Hoyle, and Jessie Wozniak for generation of *nspS* binding pocket mutant expression strains for protein purification. I greatly appreciate Dr. Chris Waters and Erik Bruger at Michigan State University for running LC-MS/MS analysis for cyclic di-GMP quantification. Many thanks go to Drs. Guichuan Hou for assistance with microscopy, Howie Neufeld for a brief schooling in statistics analysis, and the rest of the Appalachian State University Biology Department for enduring random questioning and providing intriguing conversations. Much appreciation goes to my committee members, Drs. Ted Zerucha and Darren Seals for providing support and alternative perspectives for my research questions. Finally, I would like to express deep gratitude to Dr. Ted Zerucha for suggesting my entry into graduate school under the excellent guidance and mentorship of Dr. Ece Karatan, who has since fostered my rapid development professionally and within the scientific community.

Dedication

I dedicate this work to my brothers and sisters, Steven, Devin, Katelynn, and Sonsirae, who show great potential to achieve all their hearts desire.

Table of Contents

List of Tables

List of Figures

Introduction

Biofilms

Bacterial biofilms are communities of bacteria encased in an exopolymeric substance (EPS) consisting primarily of exopolysaccharide, protein, and DNA [1-3]. Biofilms are ubiquitous in nature where these structures may form anchored to surfaces including exoskeleton of aquatic crustaceans, rocks, and glass, at liquid-air interfaces, or independently of surfaces in the form of flocs [4, 5]. In aquatic environments biofilms are often heterogeneous, and complex intercellular interactions mediate the relative composition of a variety of bacterial species [6, 7]. Symbiotic relationships also exist between biofilm forming bacteria and macroorganisms as is the case for sepiolid squid which, just hours after hatching, is colonized by *Vibrio fischeri* within crypts of the light organ [8]. The light organ provides an environment conducive for rapid bacterial cell proliferation, and at high cell densities, the *V. fischeri* community induces luciferase production at this site to aid in predation avoidance by squid in the form of counterillumination. Additionally, bacterial biofilms may be pathogenic as is the case for those formed on human teeth in the form of dental caries, within the lungs of cystic fibrosis patients by *Pseudomonas aeruginosa*, or at the site of surgical pin implants or catheter entry [5, 9]. Finally, in many aquatic systems, bacterial biofilms play a principal role in energy flow in nutrient cycling [10, 11].

Biofilm formation is a multi-step process which typically begins with transient attachments by planktonic bacteria at a surface, followed by permanent attachment to form a

monolayer, given the appropriate positive cues [6, 7]. Maturation of the biofilm occurs through further recruitment of other planktonic bacteria, as well as cell division by current members to form mushroom-like pillars of bacteria encased in EPS [12, 13]. The mature biofilm is characterized by a matrix of EPS-encrusted bacteria forming water-filled channels through which dissipation of waste and circulation of environmentally acquired nutrients is permitted [14, 15]. At this stage, some bacteria in the biofilm may detach in an attempt to colonize new surfaces or environments. Once established, the biofilm serves as a defensive unit for inhabitants by shielding and/or diminishing the effects of a multitude of stressors including UV radiation, osmotic and oxidative stress, predation, and antimicrobials [16-19]. Additionally, the complex structure of the biofilm permits communication between inhabitants as water-filled channels permit flow of intercellular signaling cues [15]. Finally, biofilms offer the additional advantage of increased environmental persistence exemplified by the pathogenic Shiga toxin-producing *Escherichia coli* biofilms formed in meat processing plants which have increased resistance against biocidal agents and sanitizers including quaternary ammonium compounds, peroxyacetic acid, and chlorine compounds [20].

Vibrio cholerae and cholera

Another example of a bacterium which uses biofilms to maintain environmental persistence is the human pathogen, *Vibrio cholerae*. This bacterium is a natural inhabitant of aquatic ecosystems including oceans, lakes, rivers, and estuaries, and is an endemic pathogen and causative agent of the disease cholera in Africa, Asia, India, and most recently, Haiti [21, 22]. Cholera outbreaks typically occur in a seasonal fashion with case numbers typically peaking following monsoons, and with warm sea surface temperatures associated with the

Spring and plankton blooms [23-25]. Exemplifying the capacity of *V. cholerae* to colonize and persist in new environments once introduced is the case of the cholera outbreak in Haiti which has continued for over five years. Indeed, cholera cases had not been reported in Haiti since the 1960's; however, since at least one UN worker reportedly contaminated Haitian water sources with *V. cholerae* during relief efforts for the 2010 earthquake, over 700,000 cases of cholera have been reported [26, 27]. Interestingly, a recent study showed that during a 2005 epidemic in Dhaka, peak levels of cholera cases were preceded by peak levels of *V. cholerae* serogroup O1 in a variety of environmental water sources, which in turn was followed by elevated levels of a lytic cholera bacteriophage, JSF4, in patient stool and water systems. This phage has been shown to produce a heat labile toxin with bacteriocidal effects on *V. cholerae* and may thus serve to limit cholera outbreaks and epidemics in its native waters, thus potentially providing options for phage-based treatment of water sources [24].

During interepidemic periods, *V. cholerae* has been shown to persist in aquatic environments by forming biofilms on a variety of aquatic organisms including chitinous crustaceans, plankton, copepods, insects, and aquatic plants [28-31]. *V. cholerae* has also been isolated from the feet and feathers of water fowl which may provide a conduit for colonization of otherwise uncontaminated water sources [31]. Cholera is often caused by consumption of contaminated drinking water and aquatic food sources [31, 32]. While the infectious dose of free swimming or planktonic organisms in healthy individuals is approximately 10^3-10^8, that of biofilm-associated organisms is orders of magnitude lower due to protection of the biofilm from the acidic environment of the stomach [33-35]. Additionally, the increased cell density of a biofilm as compared to planktonic counterparts enhances the infectious capacity of the former [36]. Following passage of *V. cholerae*

through the stomach and into the lower intestine, a variety of host factors trigger biofilm degradation and upregulation of virulence properties including those necessary for intestinal colonization, the toxin co-regulated pilus (TCP) and cholera toxin (CT) [34, 37]. TCP is required for intestinal colonization and permits non-biofilm cell aggregation and attachment to the intestinal epithelial crypts while CT causes cAMP dysregulation of intestinal cells resulting in efflux of chloride ions and water [32, 38]. This efflux results in the characteristic massive diarrhea and vomiting of cholera patients which leads to dehydration, and eventually death of the host if not promptly treated with rehydration therapy and replenishment of electrolytes [39]. Importantly, *V. cholerae* present in the stool of cholera patients are especially virulent [34]. Interestingly, biofilm components have also been detected in the stool of cholera patients indicating that, while a motile form of *V. cholerae* is required for virulence factor production, biofilm-associated cells may also be present within the intestine during infection [34, 38].

c-di-GMP metabolism

The principal regulator of biofilm formation is the cyclic di-nucleotide, bis-(3'-5') cyclic dimeric GMP, or c-di-GMP. The molecule was first discovered in *Gluconacetobacter xylinus* and determined to play a role in cellulose synthesis in this organism [40]. It has since been recognized as the key second messenger controlling a variety of phenotypes and processes including virulence, intracellular signaling, and cell-cycle progression [40, 41]. C-di-GMP is generated from two molecules of guanosine triphosphate (GTP) by enzymes known as diguanylate cyclases (DGC) with conserved GGDEF domains, and degraded to pGpG or guanosine monophosphate (GMP) by phosphodiesterases (PDE) with EAL or HD-GYP domains, respectively [42]. These domains are named for conserved amino acids which

have been shown to provide the enzymatic activity required for c-di-GMP metabolism. The catalytic domains are often linked to sensory domains involved in monitoring environmental as well as intracellular signals to control enzymatic activity. Some of the signals shown to modulate c-di-GMP turnover activity include molecular oxygen, amino acids, blue light, polyamines, and quorum sensing signals [43-45]. These substances typically interact with membrane protein domains exposed on the exterior of the cytoplasmic membrane, with periplasmic binding proteins, or directly influence intracellular proteins. The receptors may in turn directly metabolize c-di-GMP in the cytoplasm, interact with other proteins responsible for c-di-GMP metabolism, and/or initiate protein signaling cascades to control relative levels of c-di-GMP metabolizing proteins.

Many organisms produce large numbers of c-di-GMP-metabolizing enzymes. This observation is exemplified by the *V. cholerae* genome which encodes over 60 c-di-GMP-metabolizing proteins [46]. Elucidating the mechanisms, roles, and contribution of these proteins towards lifestyle-mediating decisions in various organisms has thus been the focus of many studies in the last two decades [40, 47-54]. With regards to c-di-GMP synthesis, functional DGCs usually have a conserved C-terminal GG(D/E)EF amino acid motif within the enzymatic domain as well as variable N-terminal domains involved in signal recognition [54]. Interestingly, a novel protein called VCA0965 in *Vibrio cholerae* was recently shown to have DGC activity despite having a GGDEF motif variant, AGDEF, in the active site, indicating that deviations from this conserved motif can sometimes be tolerated [52]. In 1987, the same year c-di-GMP was discovered, Benziman and colleagues showed that cyclization of two GTP molecules proceeds in a two-step reaction whereby each phosphodiester bond is formed following the release of pyrophosphate [55]. The catalytic

domain containing the GGDEF motif, called the active or A site, is the point of GTP docking [56]. To accommodate for the symmetric nature of cyclic dinucleotides, DGC domains form homodimers with the A sites facing one another in antiparallel orientation to facilitate the sequential enzymatic formation of phosphoester bonds through deprotonation of GTP 3' OH groups followed by nucleophilic attack at each α-phosphate [56, 57]. In contrast to the related adenylyl cyclases (AC), this dimerization is an apparent necessity for maximum catalytic activity [56]. The conserved GG(D/E)EF motif is believed to form a β-hairpin where both glycines in the GGDEF motif interact with the guanine base as well as with the β- and γ-phosphates while the glutamate residue coordinates either Mn^{2+} or Mg^{2+} cations required for activity [54, 56]. The third amino acid in the motif (Asp/Glu) is also believed to direct metal binding. Following release of the first pyrophosphate, a 5'-pppGpG intermediate is formed before the second round of GTPase activity occurs and the second phosphoester bond is formed resulting in the final c-di-GMP product. Interestingly, it has been shown that purified GGDEF domains form homodimers which tend to have low level DGC activity *in vitro* [58]. However, it is hypothesized that only small conformational changes occur in the A site of each homodimer subunit during c-di-GMP synthesis suggesting that the catalytic domains (if not entire monomers) remain separated until otherwise preventative regulatory mechanisms allow for an interaction to occur following recognition of a ligand/signal by the sensory domain [58]. Phosphorylation-mediated activation of response regulator (RR) DGCs by cognate sensor histidine kinases (HK) has been implicated as the most common route for formation of catalytically active homodimers [56].

Degradation of c-di-GMP in bacteria is achieved through PDE activity of proteins containing domains with conserved EAL or HD-GYP motifs [54]. The EAL domain proteins

hydrolyze c-di-GMP to 5'-pGpG and require two Mn^{2+} or Mg^{2+} molecules for catalytic activity [59]. While EAL domain proteins have been shown to break down 5'-pGpG further to two molecules of GMP, the rate of hydrolysis is much lower [60]. Similar to DGCs, EAL domain PDE dimer formation appears necessary for activation by environmental stimuli *in vitro*. Interestingly these PDEs may also form larger oligomers and show only reduced activity as monomers *in vitro* [60, 61]. Further degradation to pG (GMP) is performed by a Ca-independent enzyme. Many EAL PDEs retain some catalytic activity as monomers [54]. However, for EAL proteins to become fully active, they dimerize in an antiparallel fashion with associative interactions occurring through one α-helix from each catalytic domain and a third formed by joining two short helices from each domain [62]. When c-di-GMP enters the active site of PDE dimers, it assumes an extended or "open" shape such that phosphoester cleavage is favored. Two metal cation catalytic clusters are responsible for coordinating two water molecules in the EAL active site [62]. One of these water molecules is involved in the phosphoester bond cleavage. Optimum conditions occur at higher pH using Mn^{2+} while less optimal conditions occur with low pH and Mg^{2+} cations. Upon stimulation, conformational changes in the sensory domain impart proximity adjustments at the interface of the dimerized catalytic domain interface and in turn coordinate the metal-water cluster for optimal hydrolysis of c-di-GMP via nucleophilic attack at the phosphorus atom [62].

The second class of PDEs contains a conserved HD-GYP motif. Shortly after their discovery, these proteins were predicted to have c-di-GMP-specific hydrolytic function based on the proximity of these conserved domains to GGDEF domains which resembled the tandem GGDEF-EAL trend seen in many bacteria [54]. In support of this, it was shown by Ryan and colleagues that HD-GYP could compliment an EAL domain mutant and was

shown to specifically degrade c-di-GMP in vitro [63]. However, in contrast to EAL proteins, the final product of c-di-GMP catabolism is two molecules of GMP with pGpG as an intermediate [63]. The crystal structures of several active HD-GYP domain proteins were recently solved including Bd1817 from *Bdellovibrio bacteriovorus* and *Pm*GH from *Persephonella marina* [64]. It has been shown that these proteins are arranged facing one another with three iron ions arranged in a triangle to form the active site [65]. The HD portion of the motif was shown in particular to bind iron in the active site. The c-di-GMP molecule takes on a 'U' shape with the phosphates, located at the bend, interacting with the central iron molecule which in turn allows for a conserved aspartate residue to remove a proton from a neighboring water molecule leaving a hydroxide to make a nucleophilic attack on each phosphorus leaving two molecules of GMP [66]. Some HD-GYP domain-containing proteins have masked catalytic domains prior to activation. One example is PA4781 from *P. aeruginosa* which is catalytically inactive in the unphosphorylated state potentially due to veiling of the enzymatic motif by its REC domain [66].

Regulation of Vibrio cholerae biofilms by c-di-GMP

In *Vibrio cholerae* biofilms, the EPS consists primarily of *Vibrio* polysaccharide (VPS) whose synthesis is controlled through regulation of the *vps* genes [67]. The *vps* genes encode proteins that consist of structural and regulatory components of *V. cholerae* VPS. Transcription of these genes is controlled by the positive transcriptional regulators of biofilm formation, VpsT and VpsR [68]. The *vps* genes are clustered in two operons, *vpsA-K* and *vpsL-Q* [69]. A variety of signals influence *vps* transcription, and thus *V. cholerae* biofilm formation, including quorum sensing (QS) molecules, environmental stressors, and nutritional information [70]**.** These signals feed into a complex network of interconnected

pathways including but not limited to quorum sensing and c-di-GMP-mediated pathways which ultimately influence *vps* gene transcription. Downstream signaling culminates in modulation of intracellular concentrations of c-di-GMP to regulate biofilm formation via modulation of *vps* gene expression [54]. c-di-GMP acts at transcriptional, post-translational, and allosteric levels to maintain stringent control of transitions to and from motile and sessile lifestyles [40].

The QS pathway negatively regulates biofilm formation in *V. cholerae* via sensing of extracellular concentrations of two self-produced and secreted signaling molecules, cholera autoinducer -1 (CAI-1) and AI-2 [37]. At low cell density, and thus low autoinducer (AI) concentrations, sensory histidine kinases (HK) CpqS and LuxPQ are unbound to their respective AI's and act as kinases (Figure 1). Kinase activity results in phosphorylation of the histidine phosphotransferase (HPT) protein, LuxU (not shown), which in turn mediates phosphorylation of the response regulator (RR), LuxO [71]. LuxO is a σ^{54}-dependent transcriptional activator which, in its phosphorylated state, activates transcription of four redundant small regulatory RNAs (sRNA), Qrr1-4. These sRNAs act together with the small RNA chaperone Hfq to destabilize the mRNA of QS master regulator, HapR. At high cell density, CqsS and LuxQ are bound to CAI-1 and AI-2, respectively, and act as phosphatases resulting in HapR production [71]. HapR contains a DNA-binding motif and acts as a negative regulator of biofilm formation by modulating transcription of 14 DGC- and PDE-encoding genes in response to environmental cues [72]. Furthermore, HapR directly binds and decreases transcription of *vpsR* and *vpsT* genes encoding the positive regulators of biofilm formation, VpsT and VpsR. In addition, HapR negatively influences biofilm formation through direct binding of both *vps* operon promoters [1, 32].

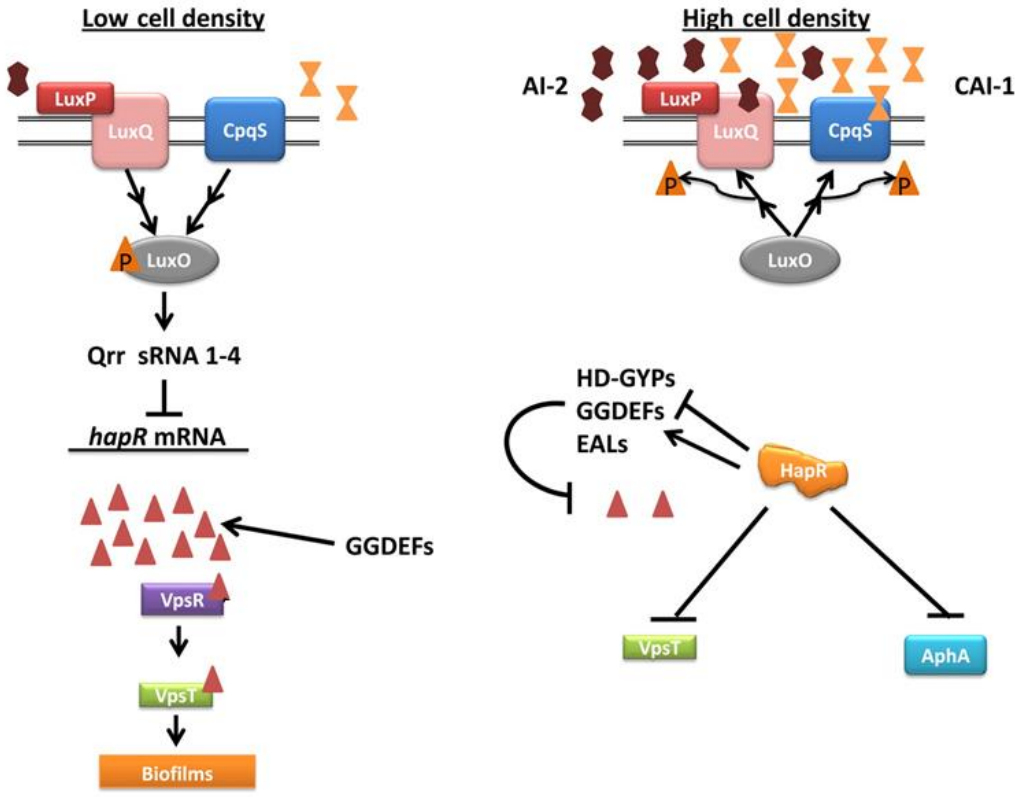

Figure 1: Quorum sensing-dependent regulation of biofilm formation. At low cell density and thus low AI concentrations, LuxPQ and CpqS remain unbound to their respective AIs, AI-2 and CAI-1, and act as kinases phosphorylating LuxO. LuxO activates Qrr sRNA 1-4 transcription which destabilizes *hapR* mRNA and permits DGC activity by GGDEF proteins allowing for accumulation of c-di-GMP (red triangles), and activation of VpsR and VpsT leading to increased biofilm formation. At high cell density, phosphoryl flow is reversed and Qrr sRNA is not made permitting HapR translation. HapR differentially regulates transcription of several DGCs and PDEs leading to reductions in c-di-GMP. Simultaneously, HapR represses VpsR and VpsT to inhibit *vps* transcription and thus biofilm formation. Adapted from [72].

The *vps* operons are under tight regulation and are controlled primarily by quorum sensing and fluctuations in intracellular c-di-GMP. Elevated levels of c-di-GMP activate VpsT and VpsR by binding these proteins. VpsT and VpsR then increase their own gene transcription as well as that of one another, several DGCs, and the *vps* genes [1]. Indeed, VpsR contains a helix-turn-helix (HTH) DNA-binding domain which, upon c-di-GMP-dependent activation, binds upstream of the *vpsT* promoter from base pair (bp) -136 to -118

in a σ^{54}-dependent manner [43]. In support of this, Casper et al. showed that VpsT expression requires VpsR [73]. However, QS inputs take precedence over c-di-GMP influences on biofilm formation as, at high cell density, QS master regulator HapR blocks *vpsT* gene transcription via binding upstream of the *vpsT* promoter in a region that overlaps the DNA-binding site of VpsR (bp -144 to -123) [43]. The same study elucidated a similar mechanism of transcriptional control for the activator of virulence gene expression, *aphA*, suggesting this may be a common theme for integrating QS- and c-di-GMP-mediated control of VPS production and virulence gene regulation [43].

While both VpsT and VpsR positively regulate VPS production, VpsR has the greatest impact on *vps* gene transcription [1]. Beyhan et al. showed that *vpsL* expression is undetectable in a *vpsR* single mutant or *vpsRhapR* double mutant and *vpsA* is transcribed at significantly lower levels as compared to that in a *vpsT* mutant [1]. Gene expression profiling, qRT-PCR, biofilm assays, and colony morphology analysis of *V. cholerae* mutants harboring all possible combinations of single, double, and triple deletion mutants of *vpsT*, *vpsR*, and *hapR* were used to generate a model for QS and c-di-GMP-mediated control of biofilm formation [1]. An epistasis model for VpsT-, VpsR-, and HapR-mediated biofilm formation has been proposed (Figure 2). As mentioned above, VpsT and VpsR positively regulate their own transcription as well as that

of one another. In addition, both proteins positively regulate transcription of the DGC, CdgA, and *vps* genes, and negatively regulate HapR. Notably, VpsR increases *cdgA* and *vps* gene transcription at a greater magnitude than VpsT [1]. In contrast, HapR negatively regulates transcription of VpsT, VpsR, CdgA, and *vps* genes as well as its own transcription.

Though not required for biofilm formation, a histidine sensor kinase, VpsS, enhances biofilm formation and overexpression of VpsS results in more robust biofilms as compared to strains expressing the same at wild type levels [74]. VpsS indirectly increases *vpsT* and *vpsR* gene transcription by funneling a phosphoryl group through the HPT and RR components of the QS circuit LuxU and LuxO, respectively. Activated LuxO then binds the promoter regions of *vpsT* and *vpsR* to increase their gene transcription [74].

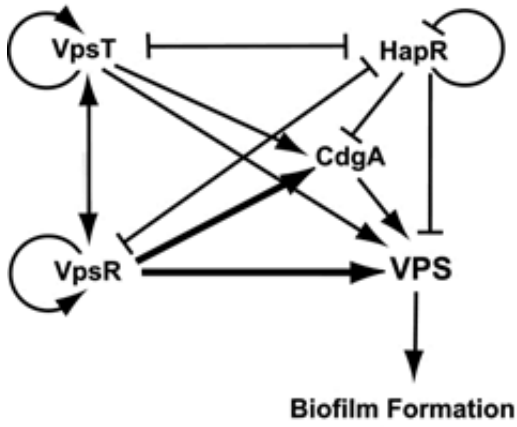

Figure 2: Biofilm formation is controlled by a complex network of transcriptional regulators. VpsT and VpsR positively regulate their own transcription, the transcription of one another, CdgA (a DGC), and that of the *vps* genes to increase biofilm formation. The contribution of VpsR to increases in CdgA and VPS gene transcription is greater than that of VpsT. The master regulator of QS, HapR, downregulates *vpsT, vpsR, cdgA, vps,* and its own transcription to decrease VPS production and biofilm formation. Thicker lines indicate greater transcriptional impact of corresponding genes [1].

Effect of polyamines on V. cholerae biofilm formation

Among the many signals known to alter *V. cholerae* biofilm formation through influences in *vps* gene transcription are polyamines; polycationic aminated hydrocarbons. Polyamines play important roles in influencing an array of cellular processes and phenotypes including growth, virulence, iron sequestration, cell wall development, acid resistance, and biofilm formation [75, 76]. The triamine norspermidine has been shown to enhance biofilm

formation in *V. cholerae* and is produced by a variety of aquatic organisms such as algae, bivalves, and plants [47, 77]. Additionally, while norspermidine is rarely produced by prokaryotes, *V. cholerae* is capable of synthesizing this polyamine which may thus serve as a *V. cholerae*-specific autoinducer signal [78]. Another triamine produced both by the host and human gut microbiota known as spermidine has been shown to inhibit biofilm formation *in vitro* suggestive of a potential role in signaling entry into the intestine to prime the bacteria for virulence factor production [79]. These effects of both of these polyamines on biofilm formation are hypothesized to occur by acting through a signaling system comprised of the proteins, NspS, short for norspermidine sensor, and MbaA [80]. Importantly, although *nspS*/*mbaA*-like gene pairs are widespread in bacteria, the *V. cholerae* NspS-MbaA signal transduction system is the first polyamine signaling system to be characterized [81]. MbaA is a transmembrane protein anchored to the cytoplasmic membrane by two transmembrane helices and contains large cytoplasmic and periplasmic domains [5]. The cytoplasmic domain is composed of a C-terminal EAL domain and membrane-proximal GGDEF domain. While wild-type *V. cholerae* forms intermediate biofilms, Δ*mbaA* mutants form robust biofilms and Δ*nspS* mutants form very little biofilms indicating that MbaA acts as a PDE in the absence of NspS [80]. In support of these observations, purified MbaA protein consisting of the cytoplasmic GGDEF and EAL domain has c-di-GMP-specific PDE activity *in vitro* [81]. Importantly, prior to this study, the contribution of MbaA to cellular c-di-GMP pools had yet to be investigated. Additionally, the potential for DGC activity has not yet been investigated for the GGDEF domain; however, it is interesting to note that the canonical GGDEF motif is degenerate and encodes an altered SGDEF motif which may render this domain inactive [81].

Future research will be required to determine if and how the GGDEF domain 1) interacts with c-di-GMP and 2) is capable of acting as a DGC.

The periplasmic domain of MbaA is hypothesized to transmit periplasmic signals by NspS through the inner membrane to control c-di-GMP metabolism. NspS is a periplasmic binding protein (PBP) homologous to the PotD protein involved in polyamine transport in *E. coli* and *V. cholerae* [80]. NspS has been shown to bind the polyamines norspermidine and spermidine, but does not play a role in transport of either polyamine indicating a potential role in signaling through MbaA [81]. There is evidence for an interaction between these proteins; however, reproducible results have been difficult to obtain, perhaps due to low expression levels of *nspS* and *mbaA* and solubility issues common with membrane proteins (Brennan WB and Karatan E, unpublished data) [82, 83].

As mentioned above, norspermidine and spermidine have opposite effects on biofilm formation in a NspS- and MbaA-dependent manner and NspS is capable of binding both polyamines *intro*. Unpublished work from our lab has identified seven conserved amino acid residues located in the binding cleft of NspS which are involved in binding of the *E. coli* PotD protein to spermidine (Figure 3) [82]. PotD is a periplasmic ligand-binding protein of the ABC-type transporter responsible for importing spermidine in *E. coli*, and is homologous to NspS. Importantly, the amino acid sequence of NspS shares greater identity with that of PotF than with PotD. PotF is another polyamine-binding protein from *E. coli*. Therefore, PotF was used for homology modeling shown in Figure 3A. From the homology model, simulations were used to identify proximal amino acids within the putative NspS binding cleft with hand-docked norspermidine which were likely to have amino-aromatic or hydrogen bond interactions with the ligand (Figure 3B). Mutation of these residues results in

drastic alterations of *V. cholerae* biofilms (Figure 3C); however, it had not been shown what effects norspermidine and spermidine have on biofilms or *vps* transcription of Δ*nspS* mutants complemented with altered *nspS* genes.

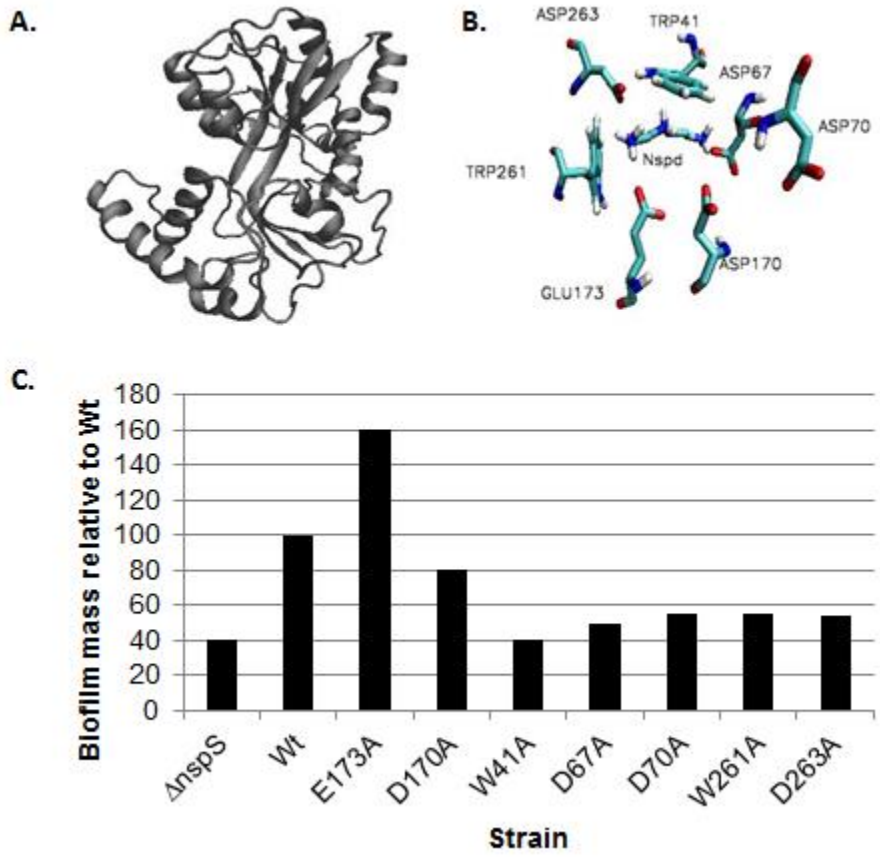

Figure 3. Conserved NspS binding pocket residues with a putative ligand-binding role influence biofilm formation. NspS homology model based off of the solved crystal structure of PotF (A). Conserved *nspS* binding pocket residues hypothesized to be involved in polyamine binding (B) were mutated and introduced into a Δ*nspS* mutant for comparison of biofilm formation to that of a strain expressing wild-type *nspS* when grown in LB media alone (C) [82].

The purpose of this study was to more thoroughly characterize the NspS-MbaA signaling system and its role in biofilm formation in response to norspermidine and spermidine. A current working model of this system composed of five points of transduction control from signal input to phenotypic output is proposed in Figure 4. In this model: 1)

norspermidine and/or spermidine in the environment enter the periplasm and interact with NspS, 2) NspS undergoes conformational changes which alter the interface between NspS and MbaA, 3) alterations at the NspS-MbaA interface modulate PDE activity in the periplasm to control c-di-GMP levels, 4) changes in intracellular c-di-GMP influence *vps* gene transcription, and 5) altered VPS production manifests in the form of altered biofilm formation.

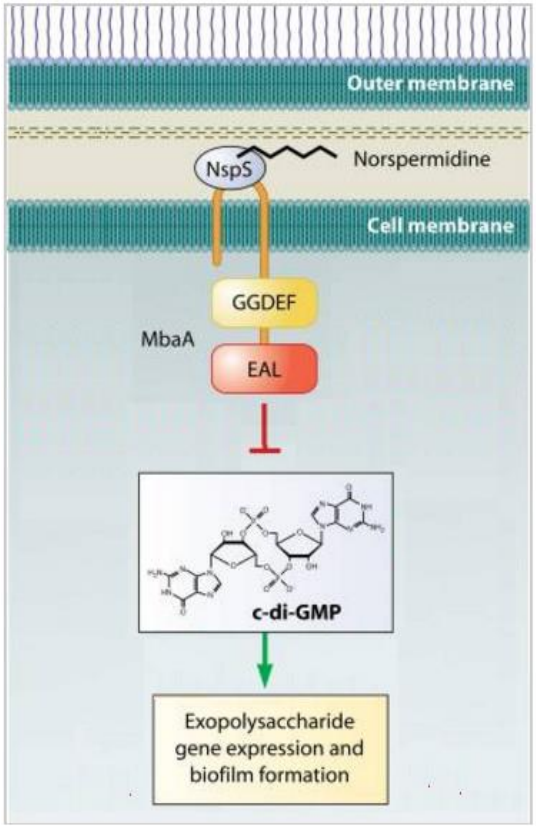

Figure 4: Schematic of the NspS-MbaA regulatory pathway. Polyamines such as norspermidine interact with NspS in the periplasm causing a conformational change at the NspS-MbaA interface to alter c-di-GMP PDE activity. Alterations in c-di-GMP influence exopolysaccharide gene expression and biofilm formation. Adapted from [5].

To further characterize the NspS-MbaA signaling system, Δ*nspS* mutants harboring altered *nspS* gene complements were investigated for their ability to alter *vps* gene transcription and biofilm formation in response to norspermidine and spermidine addition.

Additionally, binding of purified NspS mutant protein to norspermidine and spermidine was compared to that of wild-type NspS. Global c-di-GMP levels of an MbaA mutant were then quantified and compared to that of wild-type *V. cholerae*. Finally, a system for investigating the NspS-MbaA interaction as well as high through-put screening of NspS residues required for the interaction was developed.

Materials and Methods

Bacterial strains, primers, plasmids, media, and reagents

The bacterial strains and plasmids are listed in Table 1 and primers in Table 2, respectively. All strains were grown on Luria-Bertani (LB) agar (1% Tryptone, 0.5% Yeast Extract, 85 mM NaCl, 1.5 % agar) containing appropriate antibiotics for 24 hours at 37°C prior to incubation in LB or tryptone broth (1% Tryptone, 0.5%, 85 mM NaCl) and antibiotics overnight at 37°C with shaking at 200 rpm unless otherwise noted. Primer synthesis was performed by Eurofins MWG Operon (Huntsville, AL). DNA sequencing was performed by Cornell University (Ithaca, NY) and Eurofins MWG Operon (Huntsville, AL). The restriction enzymes, XhoI, SpeI, NdeI, and SalI, and Phusion and OneTaq polymerases were purchased from New England Biofilms (Beverly, MA). The polyamines, cadaverine-dihydrochloride, putrescine dihydrochloride, norspermidine, and spermidine-trihydrochloride were purchased from Sigma-Aldrich (St. Louis, MO). Chemicals and reagents were purchased from Alfa Aesar (Ward Hill, MA), Amresco (Solon, OH), Fischer Scientific (Fairlawn, NJ), Sigma-Aldrich (St. Louis, MI), or VWR (Radnor, PA) unless otherwise noted.

Visualization of nspS mutant colony morphology

Bacteria were grown on LB agar plates supplemented with 2.5µg/mL tetracycline at 27°C for 24 hours. Colonies were visualized at 25.6 x magnification using an Olympus ZX12 stereozoom microscope connected to a SONY HDR-HC7 high definition digital camcorder.

Table 1: Bacterial strains and plasmids

Strain	Genotype	Reference
***E. coli* strains**		
DH5α	F– Φ80*lac*ZΔM15 Δ(*lac*ZYA-*arg*F) 169 *rec*A1 *end*A1 *hsd*R17 (rK–, mK+) *pho*A *sup*E44 λ– *thi*-1 *gyr*A96 *rel*A1	Invitrogen
Shuffle® T7 Express	*fhuA2 lacZ::T7 gene1* [lon] *ompT ahpC gal λatt*::pNEB3-r1-*cDsbC* (Spec^R, *lacI*^{q}) Δ*trxB sulA11 R(mcr-73::miniTn10*--Tet^S)2 [dcm] *R(zgb-210::Tn10* --Tet^S) *endA1 Δgor* Δ*(mcrC-mrr)114::IS10*	New England Biolabs
AK340	Shuffle (pET28b::*nspS*$_{D170A}$)	Gardzilla A, Karatan A Unpublished data
AK350	Shuffle (pET28b::*nspS*$_{W261A}$)	Hoyle J, Karatan E Unpublished data
AK352	Shuffle (ppET28b::*nspS*$_{E173A}$)	Wozniak J, Karatan E Unpublished data
AK356	Shuffle (pET28b::*nspS*)	[84]
AK363	DH5α w/pCR2.1::*mbaA*-FLAG-0702	This study
AK369	DH5α λ pir w/pWM91::*mbaA*-FLAG-0702	This study
AK408	DH5α w/ pFLMp	This study
V. cholerae strains		
PW357	MO10, *lacZ*::*vpsL*p→ *lacZ*, Sm^r	[80]
PW444	MO10 Δ*mbaA*,*lacZ*::*vpsL*p→*lacZ*, Sm^r	[80]
PW514	MO10 Δ*nspS*, *lacZ*::*vpsL*p→*lacZ*, Sm^r	[80]
PW522	MO10 Δ*nspS*,Δ*mbaA*,*lacZ*::*vpsL*p→*lacZ*, Sm^r	[80]
AK007	PW514 (pACYC184::*nspS*)	[82]
AK035	PW514 (pACYC184::*nspS*$_{E173A}$)	[82]
AK070	PW514 (pACYC184::*nspS*$_{D170A}$)	[82]
AK075	PW514 (pACYC184::*nspS*$_{W261A}$)	[82]
AK192	PW514 (pACYC184::*nspS*)	[83]
AK193	PW522 (pACYC184::*nspS*)	This study
AK416	522 (pFLMP and pNP1)	This study
AK426	522 (pFLAG and pNP1)	This study
AK442	522 (pFLMP and pACYC184)	This study
Plasmids		
pCR2.1-TOPO	Plasmid for TOPO cloning, Ampr	Invitrogen
pFLAG-CTC	Amp	Sigma-Aldrich
pCRMP	pCR2.1::*nspS*ss-mbaAperi	This study
pFLMP	pFLAG::*nspS*ss-mbaAperi	This study

Table 2: Primers used in this study.

Primer	Description	Sequence
PA228	Forward primer for amplifying the "up" fragment of chomosomal *mbaA*-FLAG-0702	TTGCTGCACGAACTCTCGCG
PA229	Reverse primer for amplifying the "up" fragment of chomosomal *mbaA*-FLAG-0702	CTTATCGTCGTCATCCTTGTAAT CACGGCATTCACTTTGGCTGGG
PA230	Forward primer for amplifying the "down" fragment of chomosomal *mbaA*-FLAG-0702	GATTACAAGGA*TGA*CGACGATA AGTAGAAGTGCCTTTAGCACCG
PA231	Reverse primer for amplifying the "down" fragment of chomosomal *mbaA*-FLAG-0702	CTGTGCTGCGGGTGAGATGG
PA234	Reverse FLAG sequence primer to verify homologous recombination of *mbaA*-FLAG-0702	GGCTTCTACTTTGGTTATCC
PA235	Forward FLAG sequence primer to verify homologous recombination of *mbaA*-FLAG-0702	GGTTTCCTCGTCACTCAT
PA238	N26 - pFLAG-CTC forward vector primer	CATCATAACGGTTCTGGCAAATA TTC
PA239	C24 - pFLAG-CTC reverse vector primer	CTGTATCAGGCTGAAAATCTTCTC
PA253	Encodes NspS signal sequence plus six nucleotides for signal peptidase recognition with 5' *NdeI* site	CCGCCGCCATATGACCAATTTTT GTAACGAATGGGTATCGTATTCAC AAATGATCAAACGCTTTCTGTCGC TGATGGTATTGAATACTGTCTGTT ATCAAGCCAGCGCTTTGGAA
PA254	Forward primer for *nspS* signal sequence	CCGCCGCCATATGACCAA
PA255	Forward primer for *mbaA* periplasmic sequence	GTTATCAAGCCAGCGCTTTGGAA ACCAGTCAGAAAAATGCGCTGCT AA
PA256	Reverse primer for *mbaA* periplasmic sequence	GTCGACTTCGCGCTGAATGGAG TGAAGC

Biofilm assays

Overnight cultures were diluted 1:50 in fresh media (tryptone or LB) broth containing appropriate antibiotics and grown to mid-log phase at 27°C with shaking at 200 rpm. Once at mid-log phase, 1.5 mL of culture was pelleted and cells were resuspended in 150 µl fresh media. Fresh cultures were inoculated at a final OD_{595} of 0.04 in 300 µl fresh media only or media containing 10 µM, 100 µM, or 1 mM norspermidine or spermidine in borosilicate tubes. Biofilms were formed under static conditions for 48 hours at 27°C. One hundred and fifty µL of the planktonic cells were transferred to a 96-well plate for OD_{595} measurements. Biofilms were washed in 300 µL PBS and the wash was discarded. A small amount of glass beads and 300 µL PBS were added, and biofilms were sheared by vortexing for 30 seconds. Biofilm cell densities were quantified by measuring 150 µL of homogenous biofilm cell

suspension at OD_{595} in a 96-well plate. Statistical analysis was performed using two-way ANOVA through Sigma Plot.

vps gene transcription assays

vpsL promoter activity of Δ*nspS* mutants harboring a pACYC184 plasmid containing *nspS* binding pocket mutants (*nspS*$_{D170A}$, *nspS*$_{E173A}$, and *nspS*$_{W263A}$), or empty vector was compared to the same expressing wild type *nspS* in the presence and absence of spermidine by making use of a *vpsLp-lacZ* fusion in these strains. Importantly, the yeast extract of LB media contains variable levels of spermidine and thus tryptone media was chosen as the growth medium of liquid cultures in these experiments as it contains negligible amounts of spermidine (approximately 3-4 µM) (Sanders, BE and Karatan, E., unpublished data). Isolated colonies were inoculated in 2 mL tryptone media containing 100 µg/mL streptomycin and grown overnight at 27°C with shaking at 200 rpm. Day cultures were grown from overnight cultures diluted to an OD_{595} of 0.04 in fresh tryptone media in the presence or absence of 100 µM norspermidine or 1 mM spermidine. Once mid-log phase was reached, the OD_{595} was measured for standardization purposes and 1 mL of each culture was pelleted at 16,100 x g. Pellets were washed in 1 mL Z-buffer and repelleted [47]. Washed pellets were frozen at -20°C for at least 30 minutes, resuspened in 200 ul Z-buffer containing 2.7 ul/mL β-mercaptoethanol and 20 uL/mL protease inhibitors and thawed (Sigma-Aldrich, St. Louis, MO). Cells were kept cold in an ice block for the following lysis steps. Lysis was completed by three rounds of sonication on ice with a duty cycle of 30% and microtip output control of 3 for 10 seconds each. Cell debris was pelleted for 2 minutes at 16,100 x g and lysates were incubated with 40 µL of 4 mg/mL o-nitrophenyl-β-D-galactoside (ONPG) substrate at 37°C until a yellow color change was observed indicating presence of the

breakdown product of ONPG, o-nitrophenol. The OD_{415} was determined for 150 µL of the lysate-substrate mixture. Equation (1) was used to calculate Miller Units of β-galactosidase activity. Statistical analysis was performed using two-way ANOVA through Sigma Plot.

$$\text{Miller Units} = 1000*OD_{595}*(t*v*OD_{415})^{-1} \quad (1)$$

Where:

OD_{595} = Optical density of cultures

OD_{415} = Optical density of reaction mixture

t = time of reaction in minutes

v = reaction volume in mL

Purification of wild-type NspS and mutants

Overnight cultures were grown from isolated colonies resuspended in 50 µl LB broth inoculated into 20 mL LB broth with 50 mg/mL kanamycin. From overnight cultures, 10 mL were inoculated into 1 L day cultures and grown approximately 5 hours to mid-log phase. Cultures were induced with 1 mM IPTG overnight at 16°C with shaking. Cells were pelleted by centrifugation at 8,000 x g for 10 minutes at 4°C. Pellets were resuspended in 10 mL lysis buffer (50 mM NaH_2PO_4, 10 mM tris, 10 mM imidazole) and frozen at -80°C for at least 30 minutes to initiate cell lysis. Cells were thawed in cold water following addition of 20 mL lysis buffer and the protease inhibitor phenylmethanesulfonyl fluoride (PMSF) at a final concentration of 1 mM. Lysis was completed by two rounds of sonication for 60 seconds each using a microtip with a duty cycle of 40% and output control of 4. Debris was pelleted at 10,000 x g for 20 minutes at 4°C and lysates were incubated with 2 mL washed cobalt resin with end-over-end rotation for 1 hour at room temperature. The resin-lysate mixture was loaded onto a column and the resin bed was allowed to settle. Unbound fraction was

collected and the resin bed was washed by addition of 10 mL wash buffer (50 mM NaH_2PO_4, 300 mM NaCl, 10 mM imidazole). This wash was collected for downstream analysis. Proteins were then eluted in three fractions of 5 mL total elution buffer (50 mM NaH_2PO_4, 10 mM tris, 500 mM imidazole). All fractions were analyzed by SDS-PAGE. Protein was frozen at -20°C in 15% glycerol prior to use in thermal shift assays.

Thermal shift assays

Thermal shift assays (TSA) were used to determine the binding capacity of purified NspS binding pocket mutant proteins or wild type NspS protein to norspermidine or spermidine as described previously [85]. This technique works on the premise that a protein is more thermally stable when bound to its ligand. Purified wild-type NspS or $NspS_{E173A}$, $NspS_{D170A}$, or $NspS_{W261A}$ were dialyzed in TSA buffer (150 mM NaCl, 100 mM HEPES, pH 7.5) in a 3 mL Slide-a-lyzer® dialysis cassette (Thermo Scientific, Rockford, IL) once for three hours at 4°C followed by a second round of dialysis overnight at 4°C. When necessary, purified protein was concentrated using a Pierce PES 3K MWCO protein concentrator to obtain the appropriate concentration of protein. Reaction mixtures were prepared in a Microamp optical 96-well reaction plate (Thermo Scientific, Rockford, IL) with a final protein concentration of 4.75 mg/mL (8 μM), spermidine or norspermidine at 1 μM, 10 μM, or 100 μM, and SYPRO® Orange fluorescent dye (Invitrogen) at a 5x concentration. A baseline for thermal stability of protein only was established by combining purified protein, SYPRO® Orange, and TSA buffer. Negative controls containing 100 μM norspermidine and SYPRO® Orange were prepared to eliminate the possibility that an interaction was occurring between the polyamines and SYPRO® Orange dye. Additional negative controls included wild-type NspS, 100 μM cadaverine or putrescine, and SYPRO® Orange to show that the

shifts in thermal stability were specific to norspermidine and spermidine. Protein melting curves were generated by measuring fluorescence intensity of the reaction mixtures in an Applied Biosystems 7500 Real Time PCR System (Grand Island, NY). Melting temperatures (T_m) for each protein under various conditions were determined by plotting the first derivative of the fluorescent intensity against temperature using Sigma Plot and graphs were generated using Microsoft Excel 2010.

Bioinformatics

As membrane-bound proteins are prone to aggregation in aqueous solution, a novel approach for showing the NspS-MbaA protein interaction was developed. MbaA contains a large periplasmic region proposed to mediate signal transduction from the periplasm to the cytoplasm to modulate MbaA PDE activity. In order to show that MbaA interacts with NspS in the periplasm, several bioinformatics programs were used to identify the signal sequence of NspS ($NspS_{ss}$) required for periplasmic localization of the protein, and the region of MbaA localized to the periplasm ($MbaA_{peri}$). Using this information, a fusion of $NspS_{ss}$ to $MbaA_{peri}$ could theoretically be generated via splicing by overlap extension. $NspS_{ss}$ was identified by entering the known amino acid sequence into the signal peptide prediction programs SignalP 4.1 (http://www.cbs.dtu.dk/services/SignalP/), PrediSi (http://www.predisi.de/), and Phobius (http://phobius.sbc.su.se/). These programs agreed that the signal sequence likely comprised the first 33 amino acid residues (nucleotides 1-99) of NspS. $mbaA_{peri}$ was identified using several protein topology prediction programs including the TMHMM server 2.0 (http://www.cbs.dtu.dk/services/TMHMM/) and TMPred (http://www.ch.embnet.org/software/TMPRED_form.html) which identify putative transmembrane helices and provide orientation, and TOPCONS (http://topcons.cbr.su.se/) for

membrane protein topology predictions based on comparison of target protein amino acid sequences to that of solved protein structures. Altogether, these programs suggested the periplasmic region to range from amino acid 28-259 (nucleotides 82-777).

Generation of pFLMP

As determined by the bioinformatics programs described above, the $NspS_{ss}$ is encoded by the first 99 base pairs of the NspS gene. In order to express the $NspS_{ss}$-$MbaA_{peri}$ (referred to hereafter as $MbaA_p$) fusion product, a *nspS*$_{ss}$-*mbaA*$_{peri}$ construct was generated and cloned into the pFLAG-CTC expression plasmid (Sigma-Aldrich, St. Louis, MO) at *NdeI* and *SalI* restriction sites. A primer encoding the entire 99 base pair *nspS*$_{ss}$ was generated with a 5' *NdeI* site as well as several guanine and cytosine nucleotides 5' to this restriction site to bring the GC content closer to 50%. As the *NdeI* sites encodes an in-frame AUG translational start site, the native NspS start site was avoided during $NspS_{ss}$ construction (referred to hereafter as PA253). Additionally, work by Auclair et al. suggested that, because the +1 and +2 amino acids following signal peptides of proteins encoded by Gram-negative bacteria are highly conserved these amino acids are likely involved in signal peptidase I binding and cleavage [86]. Therefore, the next six nucleotides following the predicted *nspS*$_{ss}$ nucleotide sequence were added to PA253.

The primer pair PA255/256 were designed to amplify the region of *mbaA* corresponding to the nucleotides encoding the predicted periplasmic region (base pairs 28-720). PA255 also contains the last 23 base pairs of *nspS*$_{ss}$ to facilitate splicing by overlap extension, and PA256 adds a 3' *SalI* site to facilitate cloning into pFLAG-CTC. The PCR settings used included an initial denaturation for 30 seconds at 98°C, followed by 35 cycles of denaturation at 98°C for 10 seconds, primer annealing at 54°C for 20 seconds, and

extension at 72°C for 30 seconds, and concluded with a final extension step at 72°C for 10 minutes. The 692 base pair fragment was gel purified and was used in a splicing by overlap extension reaction to PA253. Following splicing, the full length *nspS*$_{ss}$-*mbaA*$_{\text{peri}}$ (referred to hereafter as *mbaA*$_p$) fragment was reamplified using a forward primer, PA254, designed to amplify from the beginning of *mbaA*$_p$, and the reverse *mbaA*$_p$ primer, PA256. The 802 base pair amplicon was verified via gel electrophoresis and PCR purified. *mbaA*$_p$ was adenylated and TOPO-cloned as according to the manufacturer's instructions, and the recombinant molecule was transformed into DH5α. The plasmid was isolated from transformants, sequenced for verification of proper sequence, and digested with *NdeI* and *SalI* to release *mbaA*$_p$. The insert was gel purified and ligated into the pFLAG-CTC expression vector linearized with the same restriction endonucleases, and the recombinant molecule, named pFLMP, was transformed into DH5α. PCR and restriction digests with *NdeI* and *SalI* were used to confirm the correct insert was present following plasmid isolation.

Expression and detection of recombinant MbaA$_p$-FLAG protein

Expression

pFLMP was electroporated into a *V. cholerae* Δ*nspS*Δ*mbaA* double mutant strain harboring a recombinant wild-type copy of *nspS* in the form of pACYC184::*nspS*, as described above, to generate AK416. To induce expression of *mbaA*$_p$, overnight cultures were diluted to an OD_{595}=0.04 in fresh media and grown to mid-log phase. Cultures were diluted 1:2 in fresh media and induced with 1 mM IPTG overnight at 37°C and cells were harvested by centrifugation for 5 minutes at 16,100 x g at room temperature. To confirm periplasmic expression of MbaAp, a periplasmic fractionation was performed via osmotic shock. Cells were resuspended in Buffer 1 (10 mM tris, 1 mM EDTA, 20% (w/v) sucrose, 4

mg/mL lysozyme) and incubated on ice for 5 minutes. The periplasm was released by addition of an equal volume of ice cold water. Cell debris was pelleted by centrifugation and the supernatant containing the periplasmic fraction was stored at -20°C for subsequent analysis by Western blotting.

Western blotting

Samples were combined with equal parts 2X Laemmli buffer and incubated in boiling water for 5 minutes prior to SDS-PAGE. Protein was transferred to a PVDF membrane in a Mini Trans-Blot® transfer apparatus (BioRad, Hercules, CA). Blots were incubated in 5% blocking buffer (PBS, 5% (w/v) skim milk) overnight at 4°C on a rotary shaker. The blot was probed with a monoclonal mouse anti-FLAG® M2- antibody conjugated to horse radish peroxidase (HRP) in 0.05% PBST for 1 hour with end-over-end rotation at room temperature. Blots were washed once for 15 minutes and twice for 5 minutes in 0.05% PBST on a rotary shaker. Chemiluminescent detection was performed by incubation for 5 minutes with Pierce^{TM} ECL western blotting substrate in the dark. Blots were imaged using a Universal Hood III system for Chemidoc MP detection system (Biorad, Hercules, CA).

In vitro crosslinking by bis(sulfosuccinimidyl) suberate (BS^3)

To investigate the NspS-MbaA interaction, it was necessary to generate the appropriate negative controls. To this end, *V. cholerae* Δ*nspS*Δ*mbaA* double mutants harboring pACYC184::*nspS*-V5 or an empty pACYC184 vector were transformed with pFLAG-CTC and pFLMP, respectively. Cultures were grown and induced as described above. Cells were harvested by centrifugation and pellets were washed three times in PBS to remove amine-containing media. Cells were resuspended in PBS and the membrane impermeable BS^3 crosslinker was added at a final concentration of 0.5, 1, 2, 3, and 4 mM.

BS3 is able to go through the outer membrane porins and localize to the periplasm; however, it cannot cross the cytoplasmic membrane. The crosslinking reaction was incubated at room temperature for 1 hour at room temperature on an end-over-end rotator prior to quenching with 20 mM Tris for 15 minutes. Cells were sonicated on ice three times for 15 seconds and cell debris was removed by centrifugation. Supernatants were stored at -20°C for further analysis.

Co-Immunoprecipitation

Following crosslinking experiments, cells were pelleted and periplasmic fractions were released as described above. Periplasmic fractions were incubated with Anti-FLAG M2 affinity beads or Anti-V5 affinity beads with end-over-end rotation at room temperature for 1 hour. The supernatant was removed and saved and beads were washed twice in PBS. Beads were resuspended in equal volumes of PBS and Laemmli buffer and samples were boiled for 5 minutes prior to SDS-PAGE. Protein was transferred to a PVDF membrane using a Mini Trans-Blot® transfer apparatus. Blots were blocked overnight in 5% (w/v) dried skim milk in PBS at 4°C. For blots whose samples were pulled down using anti-FLAG M2 affinity beads, an Anti-V5 antibody-HRP conjugate was incubated at a 1:10,000 dilution in PBS for 1 hour prior to chemiluminescent detection with the Pierce™ ECL western blotting substrate in the dark for 5 minutes. Conversely, for blots whose samples were pulled down using the Anti-V5 affinity beads, an Anti-FLAG antibody-HRP conjugate was incubated at a 1:10,000 dilution in PBS for 1 hour prior to chemiluminescent detection. A Universal Hood III system for Chemidoc MP was used to capture images of exposed blots (Biorad, Hercules, CA).

c-di-GMP quantification

Overnight cultures were diluted 1:50 in 5 mL day cultures containing LB alone, or the same supplemented with 100 μM norspermidine or 1 mM spermidine and grown to mid-log phase at 37°C with shaking. Three mL of culture were pelleted and cells were resuspended in 100 μL ice cold extraction buffer (40% methanol, 40% acetonitrile, 1 N formic acid). Tubes containing resuspended cells were sealed with parafilm and incubated at 65°C for ten minutes to ensure complete lysis. Cells were then incubated at -20°C for 30 minutes and solutions were neutralized by adding NH_4HCO_3 to a final concentration of 0.58% (w/v). Cell debris was removed by centrifugation for 5 minutes at 16,100 x g and supernatants were transferred to O-ring tubes for storage at -80°C prior to shipping on dry ice for LC-MS/MS analysis. LC-MS/MS analysis was performed by Eric Burger in Dr. Chris Waters' lab at Michigan State University using a Quattro Premier XE mass spectrometer (Waters) coupled with a Acquity Ultra Performance LC system (Waters) was used for c-di-GMP detection as described previously [46].

Expression and purification of NspS for polyclonal antibody production

To generate the NspS antibody, approximately 2 mg/mL purified NspS was needed at three 1-month intervals for injection in rabbits. Previous work with the system used in our lab to overexpress NspS revealed that the majority of protein aggregated in inclusion bodies; however, previous work has shown that inclusion bodies may be used for antibody production [87]. Therefore, this approach was chosen for producing enough protein antigen to be used for antibody generation.

In order to overexpress NspS, isolated colonies of SHuffle T7 Express *E. coli* cells harboring pET28b::*nspS* were grown overnight in LB broth at 37°C with shaking. Overnight cultures were diluted 1:1000 in 1L of LB and grown to mid-log phase under the same

conditions. Once at mid-log phase, cultures were induced overnight with 500 μM IPTG at 30°C with shaking. Cells were then harvested at 8000 x g for 20 minutes at 4°C. Cells were then resuspended in 20 mL denaturing lysis buffer (50 mM NaH_2PO_4, 10 mM tris, 8 M urea, 10 mM imidazole) and frozen at -80°C for 30 minutes. Cell lysis was initiated by thawing at room temperature with the addition of 60 mL denaturing lysis buffer for 30 minutes followed by three rounds of sonication on ice for 60 seconds each using a microtip with a duty cycle of 40% and output control of 4. Cell debris was pelleted by centrifugation at 14000 x g for 20 minutes at room temperature and the supernatant was added to 1 mL prepared HisPur™ cobalt Resin (Thermo Scientific, Rockford, IL). Cobalt resin was prepared by spinning gently at 700 x g for two minutes and washing twice in 10 mL denaturing lysis buffer. The cell lysate was incubated with cobalt resin overnight at room temperature with end-over-end rotation.

Following incubation, the resin was pelleted at room temperature for five minutes at 700 x g, resuspended in 10 mL wash buffer (50 mM NaH_2PO_4, 300 mM NaCl, 8 M urea, 10 mM imidazole), loaded on a column, and allowed to settle. Once the resin bed had collected at the bottom of the column, the wash was eluted and retained. A second wash with 10 mL lysis buffer was applied without disturbing the resin. The unbound fraction and combined washes were retained for further analysis. Bound protein was eluted with 5 mL elution buffer (50 mM NaH_2PO_4, 10 mM tris, 8 M urea, 500 mM imidazole) in five 1 mL fractions. All fractions were analyzed by SDS-PAGE prior to further processing. Inclusion bodies were precipitated by dialysis in a Slide-a-lyzer® dialysis cassette (Thermo Scientific, Rockford, IL) at 4°C for 6 hours in PBS. Inclusions were pelletted and washed twice in inclusion body wash buffer (137 mM NaCl, 2.7 mM KCl, 10 mM Na_2HPO_4, 2 mM KH_2PO_4, 1 M urea, pH

7.4) and once in PBS prior to resuspension in PBS and storage at -20°C for antibody production. A male New Zealand white rabbit was immunized over an eleven week course at weeks 0, 3, 6, 9, and 11 with an emulsion of 0.5 ml of 2 mg/mL antigen in PBS and 0.5 mL of Freund's Complete Adjuvant (Sigma). The rabbit was sacrificed at week 12 and whole serum was separated from blood cells by allowing the latter to clot overnight. Whole serum was aliquoted and stored at -20°C prior to purification.

Testing of polyclonal Anti-NspS antibodies via Western blot and ELISA

Purification of Anti-NspS antibody

Whole rabbit serum was purified using a Melon^{TM} Gel IgG spin purification kit from Thermo Fisher Scientific (Carlsbad, CA) according to the manufacturer's instructions. Purified antibody was aliquoted and stored at -20°C for later use. Purified antibody was compared to whole serum via SDS-PAGE and Coomassie staining analysis.

Western blotting with the Anti-NspS antibody

Overnight cultures were pelleted and resuspended in PBS with 20 µL/mL protease inhibitors (Sigma-Aldrich, St. Louis, MO). Cells were sonicated on ice three times and debris was pelleted by centrifugation at 16,100 x g for 20 minutes at 4°C. Lysates were run via SDS-PAGE and protein was transferred to PVDF membrane in a Mini Trans-Blot® transfer apparatus. Following transfer, blots were blocked overnight in 5% (w/v) skim milk in PBS at 4°C. Blots were incubated with purified anti-NspS antibody at a final concentration of 1 µg/mL in 3% (w/v) skim milk in 0.05% PBST for 1 hour at room temperature, washed three times in 0.05% PBST for 5 minutes each, and incubated with goat anti-rabbit-HRP antibody conjugate at a 1:10,000 dilution in PBST for 1 hour with end-over-end rotation at room temperature. Blots were washed once for 15 minutes in 0.05% PBST followed by two more

washes in the same for 5 minutes each. Chemiluminescent detection was performed as described above.

NspS ELISA

To test the anti-NspS antibody efficacy in ELISA experiments, high affinity microtiter plates were coated with anti-NspS capture antibody at 1 μg/mL in carbonate buffer pH 9.6 overnight at 4°C. On the next day, coating solution was removed and the plate was washed twice with PBS, and plates were blocked with 5% (w/v) dried skim milk in 0.05% PBST for 2 hours at room temperature. Periplasmic extracts or whole cell lysates, prepared by sonication or using Bugbuster® Protein Extraction Reagent (Thermo Scientific, Waltham, MA), from AK192 or AK007 were added to wells in sequential 1:2 dilutions and incubated 2 hours at room temperature for capture. Wells were washed four times with PBS and Anti-V5 antibody-HRP conjugate was added at a 1:1000 dilution in PBST for 1 hour. The plate was washed four times with PBST and incubated with 3, 3', 5, 5'-tetramethylbensidine (TMB) substrate for 10 minutes in the dark. Reactions were stopped by adding an equal volume of phosphoric acid prior to measuring the OD_{450}.

Results

Mutations in the NspS binding cleft alter polyamine-mediated influences on biofilm formation

NspS has been shown to have a positive influence on biofilm formation (Karatan et al. 2005), and mutation of specific binding pocket residues hypothesized to be involved in mediating polyamine binding has severe impacts on biofilm formation *in vitro* [82]. Additionally, the polyamines norspermidine and spermidine have been shown to increase and decrease biofilm formation of wild type *V. cholerae*, respectively, in a *nspS*-dependent manner. Therefore, it was hypothesized that addition of these polyamines would have less, if any, influence on polyamine-mediated biofilm formation by strains producing NspS binding pocket mutants. Three strains expressing *nspS* with putative ligand-binding residue mutations to alanine were chosen for further analysis; these residues include Glu173, Asp170, and Trp261.

To test the impact of binding cleft mutations on NspS-mediated signaling in response to norspermidine, mid-log phase cultures were diluted to an OD_{595} of 0.04 in fresh tryptone or LB media only, or in the presence of increasing concentrations of norspermidine (10 μM, 100 μM, or 1 mM). As LB contains variable levels of spermidine (approximately 10-40 μM), these experiments were performed in both, LB and tryptone media to determine what differences may be observed for biofilm formation in these media types. Cultures were grown statically for 48 hours at which point biofilms were dispersed with glass beads and

vortexing, and biofilm cell density was measured (Figure 5). Addition of norspermidine to culture medium had a statistically significant positive influence on strains harboring wild-type NspS when grown in both tryptone broth (Figure 5A) and LB media (Figure 5B), while the Δ*nspS* mutant formed little to no biofilms under these conditions regardless of the growth medium. Interestingly, the *nspS*$_{E173A}$ mutant formed robust biofilms comparable to wild-type in tryptone media, or greater than wild type in LB, but did not respond to norspermidine addition. In contrast, *nspS*$_{D170A}$ and *nspS*$_{W261A}$ formed very low biofilms in media alone. At both 100 µM and 1 mM norspermidine, both strains formed very robust biofilms comparable to both wild-type and the *nspS*$_{E173A}$ mutant. However, *nspS*$_{W261A}$ did not respond to the lower concentration of 10 µM norspermidine, while *nspS*$_{D170A}$ doubled its biofilm mass at this concentration. Notably, strains expressing wild-type *nspS*, *nspS*$_{D170A}$, or *nspS*$_{W261A}$ all show a slight decrease in biofilm formation at 1 mM norspermidine as compared to 100 µM norspermidine when grown in tryptone broth. Another perhaps less surprising observation is that all strains grew much more slowly in tryptone broth (OD_{595}=0.2 for untreated wild-type cultures) as compared to the more complex LB medium (OD_{595}=0.3 for untreated wild-type cultures), regardless of polyamine addition (Figure 6A and B). In comparing LB, the ratios of planktonic to biofilm cells appear to compensate one another *i.e.* as cells partition into the biofilm fraction, planktonic cell density decreases noticeably. In contrast, partitioning of cells from the planktonic fraction is less noticeable for cultures grown in tryptone. This may be due to the decreased growth rate of these cultures as compared to those grown in LB. Altogether, these data indicate that the varying polyamine conditions used in these assays did not appear to impart a growth defect for any given strain.

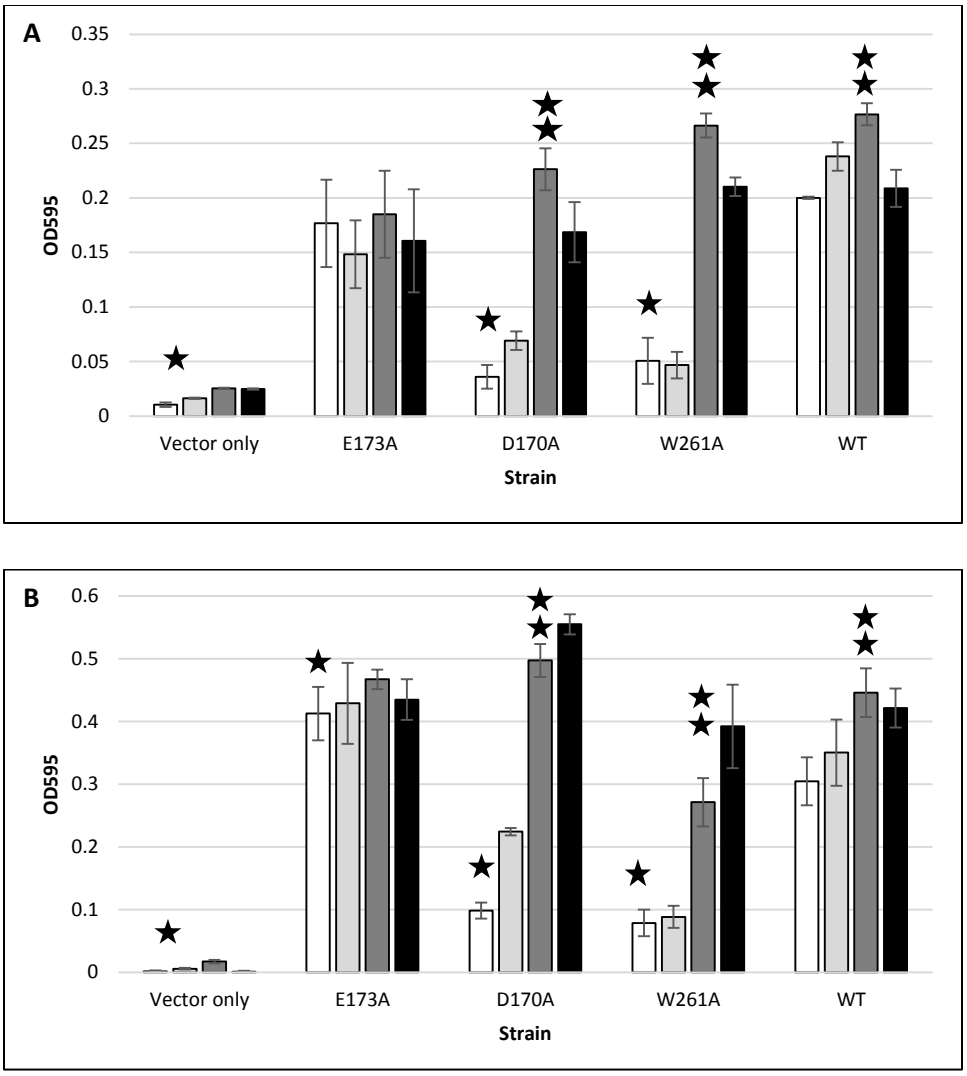

Figure 5: Biofilm formation in media alone or with increasing concentrations of norspermidine. Biofilm formation was compared for Δ*nspS* mutants with pACYC184 vector only, or complemented with $nspS_{E173A}$, $nspS_{D170A}$, $nspS_{W261A}$, or wild-type (WT) *nspS*. Mid-log cells were diluted to an OD_{595} of 0.04 in fresh tryptone (A) or LB (B) alone (white bars) or supplemented with various concentrations of norspermidine. Norspermidine concentrations include 10 µM (light grey bars), 100 µM (dark grey bars), and 1 mM (black bars). Following 48 hours of static incubation at 27°C, planktonic cells were removed and biofilms were sheared with glass beads and vortexing. Biofilm cell density was measured at OD_{595}. Single stars indicate significant differences compared to wild-type cultures grown in the absence of norspermidine ($p<0.05$). Double stars indicate significant differences of biofilm formation for the specific strain and treatment as compared to the same strain without norspermidine addition. Error bars show standard deviation of three biological replicates ($p<0.05$). Statistical analysis was performed using two-way ANOVA in Sigma Plot.

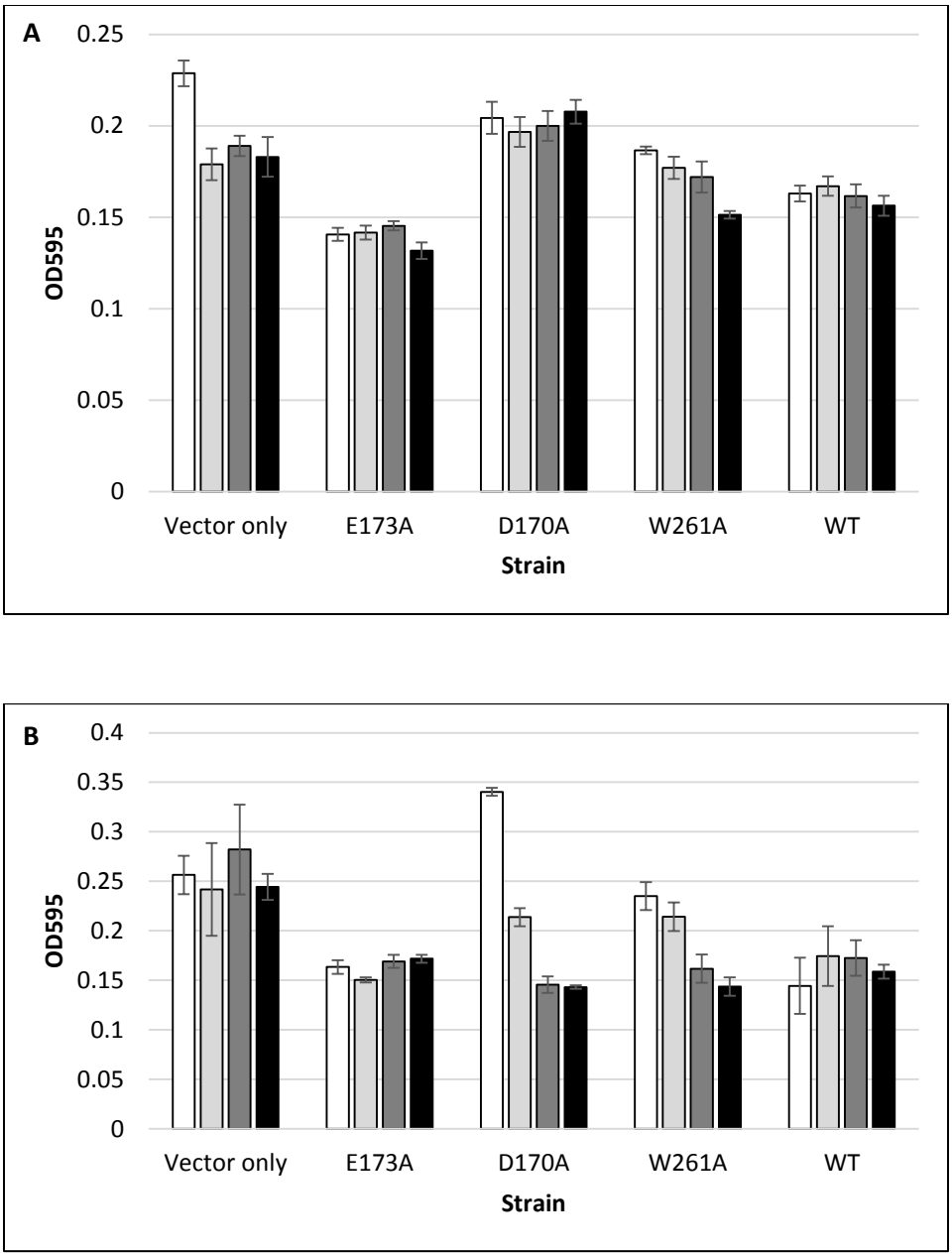

Figure 6: Planktonic growth in media alone or with increasing concentrations of norspermidine. Planktonic cell growth was compared for Δ*nspS* mutants with pACYC184 vector only, or complemented with $nspS_{E173A}$, $nspS_{D170A}$, $nspS_{W261A}$, or wild-type (WT) *nspS*. Mid-log cells were diluted to an OD_{595} of 0.04 in fresh tryptone (A) or LB (B) alone (white bars) or supplemented with various concentrations of spermidine. Norspermidine concentrations include 10 µM (light grey bars), 100 µM (dark grey bars), and 1 mM (black bars). Following 48 hours of static incubation at 27°C, planktonic cells were removed and measured at an OD_{595}. Error bars show standard deviation of three biological replicates ($p<0.05$).

The impact of NspS binding pocket mutants on biofilm responsiveness to spermidine addition was also tested for cultures grown in tryptone or LB media using the same concentrations described for norspermidine (Figure 7). Again, Δ*nspS* mutants harboring a wild-type *nspS* complement formed increased biofilms when grown in media alone as compared to the vector-only control which was unresponsive at all concentrations of spermidine. As seen previously, spermidine addition did not significantly influence wild-type strains until concentrations reached 1 mM at which point a decrease of about 25% in biofilm formation was observed in either medium. In contrast, and similar to observations made with norspermidine, the $nspS_{E173A}$ mutant was unresponsive to spermidine addition at all concentrations when grown in LB media. However, when grown in tryptone, the same mutant responded with a significant increase in biofilm formation in the presence of 100 µM spermidine, but biofilm formation was repressed back to levels seen in the absence of this polyamine when grown in the presence of 1000 µM spermidine. This observation suggests that other players may be contributing additively biofilm formation in response to this polyamine. Contrary to observations with norspermidine, $nspS_{W261A}$ did not respond to any concentration of spermidine and maintained a relatively low biofilm cell density under all conditions. Notably, $nspS_{D170A}$ showed a slight yet significant decrease in biofilm formation in the presence of 1 mM spermidine in both tryptone and LB. Again, all strains grew much more rapidly in LB medium than tryptone broth regardless of polyamine addition (Figure 8A and B, respectively) and increased partitioning to biofilms in LB resulted in a noticeable compensatory decrease in planktonic cell density such that strains which grew increased biofilms had yielded fewer numbers in the planktonic fraction. Altogether, biofilm observations show that the conserved binding pocket residue E173 may be important for

norspermidine and spermidine-mediated control of biofilms while D170 and W261 may be necessary for signaling by spermidine alone.

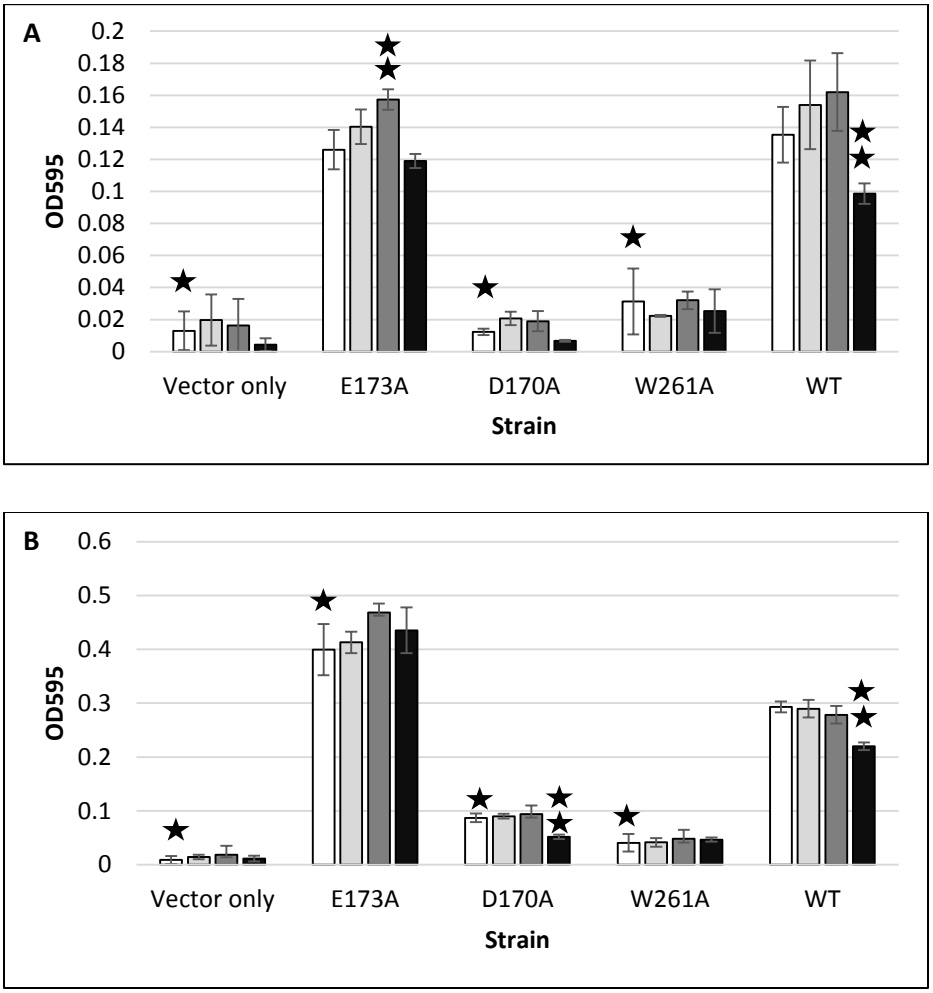

Figure 7: Biofilm formation in media alone or with increasing concentrations of spermidine. Biofilm formation was compared for Δ*nspS* mutants with pACYC184 vector only, or complemented with $nspS_{E173A}$, $nspS_{D170A}$, $nspS_{W261A}$, or wild-type (WT) *nspS*. Mid-log cells were diluted to an OD_{595} of 0.04 in fresh tryptone (A) or LB (B) alone (white bars) or supplemented with various concentrations of spermidine. Spermidine concentrations include 10 µM (light grey bars), 100 µM (dark grey bars), and 1 mM (black bars). Following 48 hours of static incubation at 27°C, planktonic cells were removed and biofilms were sheared with glass beads and vortexing. Biofilm cell density was measured at OD_{595}. Single stars indicate significant differences compared to wild-type cultures grown in the absence of spermidine Double stars indicate significant differences of biofilm formation for the specific strain and treatment as compared to the same strain without spermidine addition. Error bars show standard deviation of three biological replicates ($p<0.05$). Statistical analysis was performed using two-way ANOVA in Sigma Plot.

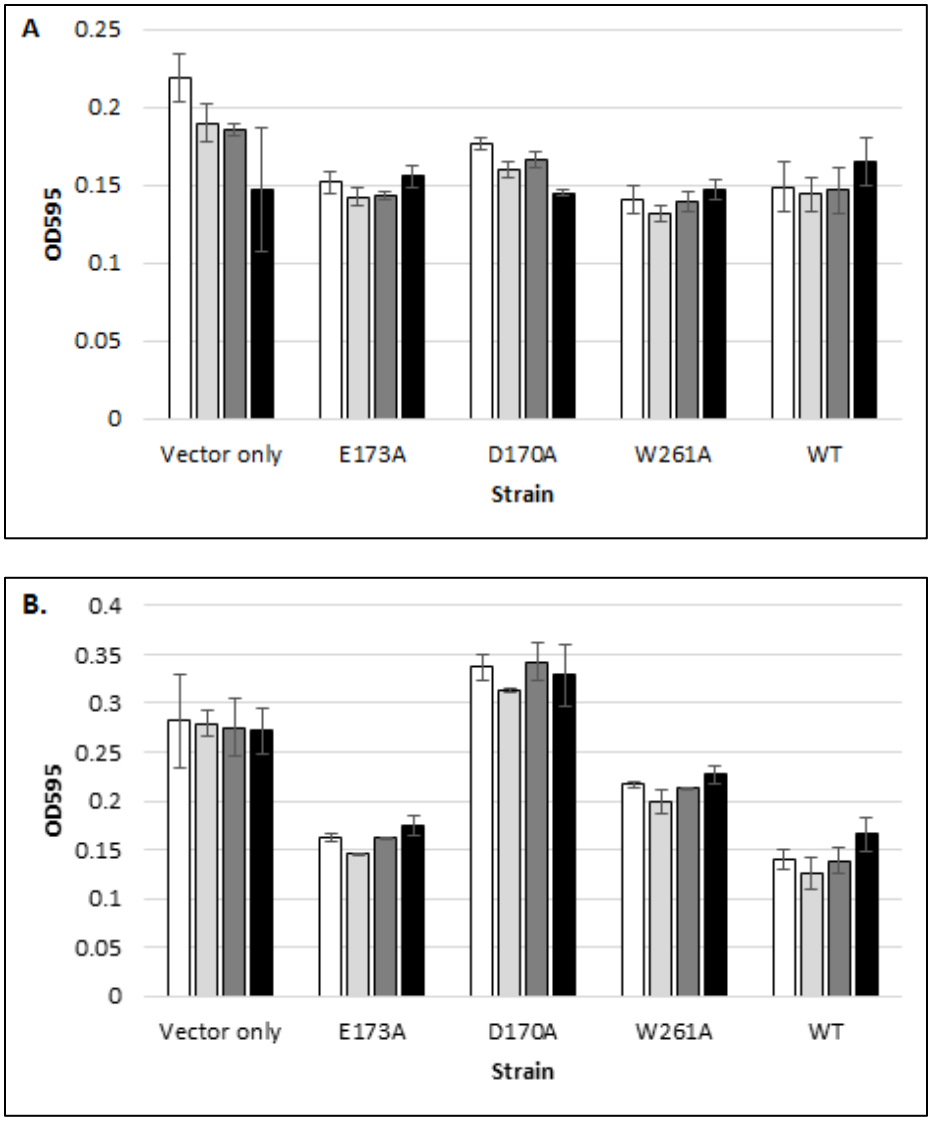

Figure 8: Planktonic growth in media alone or with increasing concentrations of spermidine. Planktonic cell growth was compared for Δ*nspS* mutants with pACYC184 vector only, or complemented with $nspS_{E173A}$, $nspS_{D170A}$, $nspS_{W261A}$, or wild-type (WT) *nspS*. Mid-log cells were diluted to an OD_{595} of 0.04 in fresh tryptone (A) or LB (B) alone (white bars) or supplemented with various concentrations of spermidine. Spermidine concentrations include 10 µM (light grey bars), 100 µM (dark grey bars), and 1 mM (black bars). Following 48 hours of static incubation at 27°C, planktonic cells were removed and measured at an OD_{595}. Error bars show standard deviation of three biological replicates ($p<0.05$).

NspS ligand-binding pocket mutants have altered colony morphologies

I hypothesized that the increased biofilm phenotype noted for *nspS* mutants grown in LB static cultures may be the results of increased VPS production which has been shown previously to result in corrugated or rugose colony morphology. However, it was noted that even in the absence of polyamines colony morphology of *nspS* binding-binding pocket mutants on LB media differed noticeably from that of wild-type *V. cholerae* (Figure 9). While Δ*nspS* mutant strains containing vector only, $nspS_{D170A,}$ or $nspS_{W261A}$ produced comparatively smooth colonies, the $nspS_{E173A}$ mutant formed wrinkly colonies indicative of increased polysaccharide content as compared to the intermediate rugose appearance of that expressing wild-type *nspS*.

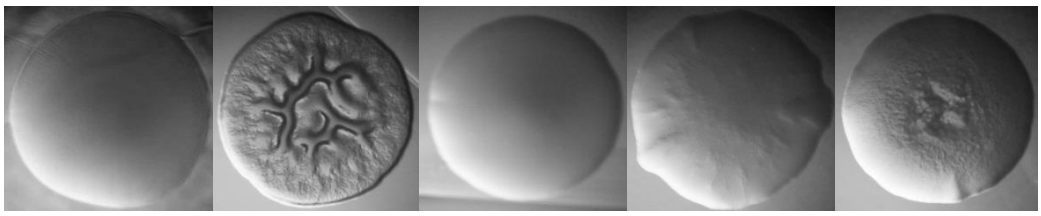

Figure 9: Colony morphologies of *nspS* ligand-binding pocket mutants. *V. cholerae* Δ*nspS* mutants harboring a pACYC184 vector alone, or with wild-type *nspS* or *nspS* ligand-binding pocket mutants were grown on LB agar with 2.5 µg/mL tetracycline for 24 hours prior to imaging through an Olympus SZ12 stereoscope at 25.6 x magnification. From left to right, *nspS* mutants were complemented with: vector only, $nspS_{E173A}$, $nspS_{D170A}$, $nspS_{W261A}$, and wild-type *nspS*.

Mutations in the NspS ligand-binding cleft alter polyamine-mediated influences on vps transcription

V. cholerae biofilm matrix is largely composed of polysaccharide, extracellular DNA, and protein. The production and export of the polysaccharide component is dependent upon transcription of *Vibrio* polysaccharide (VPS) genes located within two clusters (*vps*I and *vps*II) on the large chromosome consisting of *vpsA-K* and *vpsL-Q*. Previous research in our lab has shown that *vpsL* promoter activity is increased in wild-type strains grown in the

presence of as little as 10-30 µM norspermidine, and that these effects are abolished in a Δ*nspS* mutant. Therefore, to investigate whether the biofilm phenotypes observed for *nspS* ligand-binding pocket mutants were a direct result of altered *vps* gene transcription, β-galactosidase assays were performed making use of a chromosomal $vpsL_p$-*lacZ* fusion in the Δ*nspS* background (Figure 10). Using this construct, one can correlate β-galactosidase activity to *vpsL* promoter activity by adding a colorimetric substrate, o-nitrophenyl-β-galactoside (ONPG), to cell lysates. Production of the derivative product of ONPG, o-nitrophenol, results in a yellow color change which can be quantified at an OD_{415}. To this end, overnight cultures were diluted to an OD_{595} of 0.04 in fresh tryptone media only, or in the presence of 100 µM norspermidine or 1 mM spermidine and grown statically to mid-log phase. The OD_{595} of planktonic cells was recorded for standardization and pelleted. Cells were washed once in Z-buffer, pellets were frozen to initiate lysis, and cells were resuspended in the same to complete lysis by sonication. Cell debris was pelleted and ONPG was added to lysates until a color change was observed.

As seen in Figure 11, a slight increase in $vpsL_p$ activity was observed for strains harboring wild-type *nspS* when grown in the presence of norspermidine; however, this difference was not statistically significant under the conditions tested. In contrast, a statistically significant decrease was observed for the same in spermidine-containing media. Very low $vpsL_p$ activity was observed for the Δ*nspS* mutant under all conditions. As expected based on observations made for biofilms by this strain, the $nspS_{E173A}$ mutant showed high transcription from $vpsL_p$ in tryptone alone and was unresponsive to both, norspermidine and spermidine. Additionally, $nspS_{W261A}$ showed initially low $vpsL_p$ transcription, but a

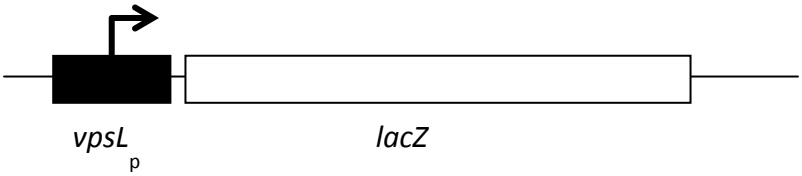

Figure 10: Diagram of the chromosomal *vpsL*$_p$-*lacZ* fusion used for *vps* assays.

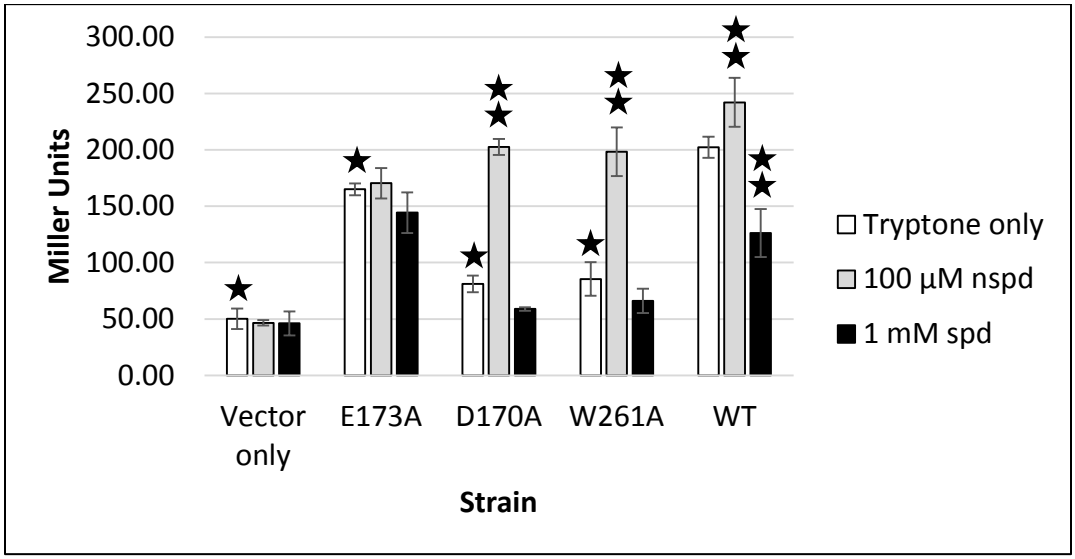

Figure 11: *vpsL* transcription in media alone or in the presence of 100 µM norspermidine (nspd) or 1 mM spermidine (spd). *Vps* transcription was compared for Δ*nspS* mutants with pACYC184 vector only, or complemented with *nspS*$_{E173A}$, *nspS*$_{D170A}$, *nspS*$_{W261A}$, or wild-type (WT) *nspS*. Overnight cultures were diluted to OD_{595} of 0.04 in fresh tryptone media only (white bars), or media containing 100 µM norspermidine (grey bars) or 1 mM spermidine (black bars) and grown to mid-log phase. Cells were harvested for washing and lysed by sonication prior to incubation of the lysate with ONPG. Miller units of β-galactosidase activity were calculated as described in Materials and Methods. Single stars indicate significant differences compared to wild-type cultures grown in the absence of spermidine (p<0.05). Double stars indicate significant differences of Miller units for the specific strain and treatment as compared to the same strain without polyamine addition. Error bars show standard deviation of three biological replicates (p<0.05). Statistical analysis was performed using two-way ANOVA in Sigma Plot.

significant positive *vpsL*$_p$ transcriptional response to norspermidine while spermidine had no apparent effect. Further corroborating biofilm observations, *vpsL* promoter activity was low for *nspS*$_{D170A}$ in tryptone alone, but responded with over a two-fold increase to norspermidine, and a slight, yet insignificant decrease to spermidine addition. These data indicate that the altered biofilm phenotypes observed for *nspS* ligand-binding pocket mutants

in the presence or absence of norspermidine and spermidine are a direct result of altered *vps* gene transcription imparted by these mutants.

Global c-di-GMP pools are unaffected by norspermidine and spermidine or presence of NspS and MbaA

MbaA is confirmed to have PDE activity *in vitro* which is unchecked in the absence of NspS leading to degradation of c-di-GMP, and reduction of *vps* transcription and biofilm formation [81]. To determine if cellular c-di-GMP pools are affected by signal transduction mediated by NspS in the presence or absence of norspermidine or spermidine, wild-type *V. cholerae* or a Δ*nspS* mutant were grown to mid-log phase in media only or in the presence of 100 μM norspermidine or 1 mM spermidine. c-di-GMP was extracted and quantified as described previously [46]. As shown in Figure 12, c-di-GMP levels are maintained at approximately 45-65 nM regardless of polyamine concentration, or presence of NspS indicative of a high specificity signaling system.

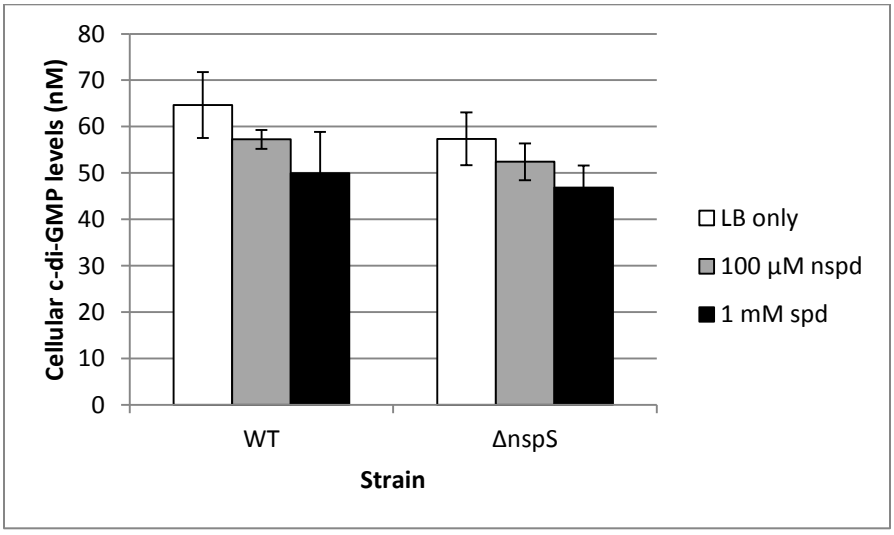

Figure 12: Cellular c-di-GMP levels of Δ*nspS* mutants in the presence and absence of norspermidine (nspd) or spermidine (spd) compared to wild-type (WT). Overnight cultures were diluted 1:50 in fresh media with alone or supplemented with 100 μM nspd or 1 mM spd and grown to mid-log phase. c-di-GMP was extracted as described in Materials and Methods and quantified by LC-MS/MS. Error bars show standard deviation of three biological replicates ($p<0.05$).

Purification of wild-type NspS and ligand-binding pocket mutants

The current working model for norspermidine- and spermidine-mediated signaling through NspS requires that NspS directly interacts with either polyamine within the periplasm causing a conformational change in NspS which induces or alters an interaction between NspS and MbaA. This signal is then transmitted to the cytoplasmic domains of the latter to influence PDE activity, alter some pool of c-di-GMP, and influence *vps* transcriptional activity to control biofilm formation. Therefore, it was hypothesized that alterations at proposed NspS ligand-binding pocket residues would in turn hinder the ability of NspS to bind norspermidine and/or spermidine. Previously, it was shown using thermal shift assays (TSA) that purified wild-type NspS is capable of binding norspermidine and spermidine, but not other polyamines, specifically putrescine and cadaverine [81].

In an effort to determine the affinity of the binding pocket mutants to norspermidine and spermidine, the wild-type or the altered NspS proteins were purified using an *E. coli*-based expression system. Wild-type or mutant *nspS* genes, each lacking the periplasmic signal sequence, were expressed from a pET28b plasmid under the control of the IPTG-inducible *lac* promoter. Additionally, the pET28b plasmid adds a 6-Histidine (6-His) tag which has a high affinity for Co^{2+} permitting protein purification. Previous work in our lab has shown that optimal soluble *nspS* expression may be achieved by overnight induction of mid-log phase cultures with 1 mM IPTG. A second screen was used to determine that increased soluble protein recovery could be achieved by inducing overnight at 16°C as opposed to 30°C. Cells were harvested by centrifugation and lysed by one freeze-thaw cycle followed by sonication. The 40 kDa NspS protein was purified using a Co^{2+} resin and analyzed by SDS-PAGE and Coomassie staining (Figure 13). Panel A shows the wild-type NspS fractions

(lanes 2-7) including whole cell lysate (WCL), unbound fraction (UBF), wash (W), and elutions (E1-3). $NspS_{D170A}$ fractions are present on Panel A (lane 8-10) and Panel B (lane 1-3). $NspS_{W261A}$ fractions are shown in Panel B (lane 5-10) and $NspS_{E173A}$ samples are shown in Panel C. As shown in Figure 13, all elutions contained large amounts of purified wild-type or mutant protein.

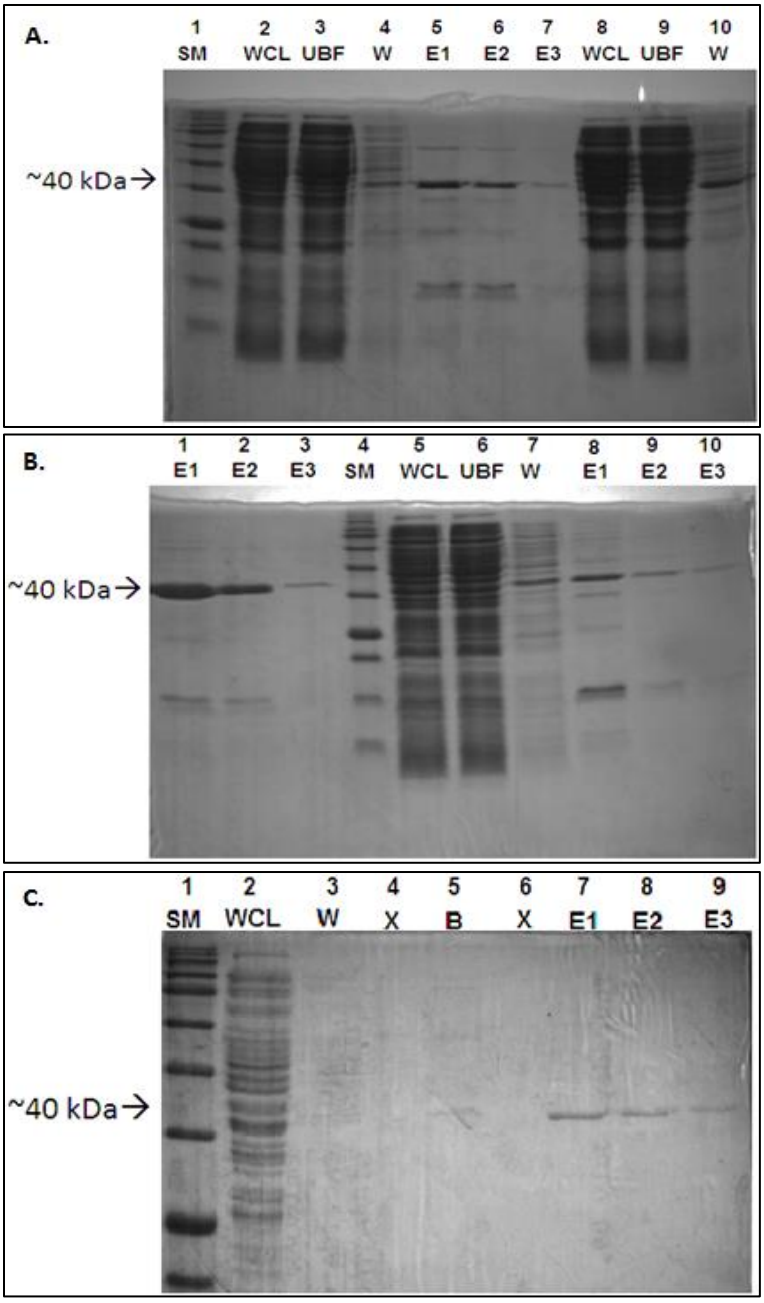

Figure 13: Purification of recombinant NspS proteins. Mid-log cultures were induced overnight at 16°C with 1 mM IPTG. Cells were harvested, lysed, and the supernatants were bound to Co^{2+} resin at room temperature for 1 hour. The resin was washed and bound protein was eluted in three fractions. Protein samples were run via SDS-PAGE on three gels as follows: Panel A Lane 2-7 wild-type NspS, Panel A Lane 8-10 and Panel B Lane 1-3 $NspS_{D170A}$, Panel B Lane 5-10 $NspS_{W261A}$, Panel C Lane 2, 3, 5, 7-9 $NspS_{D173A}$. Legend: SM – size marker, WCL – whole cell lysate, UBF – unbound fraction, W – wash, E – elution, B – beads, X – buffer lane.

NspS ligand-binding pocket mutants maintain the capacity to bind norspermidine and spermidine

To compare the thermal stability profile of purified wild-type or mutant NspS protein in the presence of increasing concentrations of norspermidine or spermidine to that of protein alone, TSAs were performed. These experiments work on the principal that binding proteins are more thermally stable when bound to a ligand. Reaction mixtures consist of target protein, a fluorescent dye such as SYPRO Orange®, and a putative ligand. SYPRO® Orange nonspecifically binds hydrophobic surfaces and residues leading to increased fluorescence while aqueous solution quenches said fluorescence. Therefore, as the reaction mixture is heated in a stepwise manner, protein begins to unfold and the hydrophobic interior becomes exposed resulting in increased SYPRO® Orange binding to the protein and increased fluorescence. By plotting the rate of change of fluorescence intensity as a function of temperature, the T_m of the protein may be determined where T_m is the temperature at which the rate of change of fluorescence intensity is at its maximum.

It was previously determined using TSAs that purified wild-type NspS interacts specifically with norspermidine and spermidine, but not cadaverine or putrescine [81]. To further support these observations, a control was performed with NspS protein alone, or in the presence of 100 μM norspermidine, cadaverine, or putrescine (Figure 14). Indeed, while an 8°C shift in the T_m was observed for NspS in the presence of norspermidine as compared to protein only, neither putrescine nor cadaverine influenced NspS stability indicating lack of a binding event for these latter polyamines. However, as seen in Figure 15, addition of as little as 1 μM norspermidine or spermidine resulted in a 2-3°C shift in thermal stability while

10µM and 100 µM norspermidine and spermidine resulted in about 5-6°C and 7-8° shifts for the respective concentrations compared to protein alone.

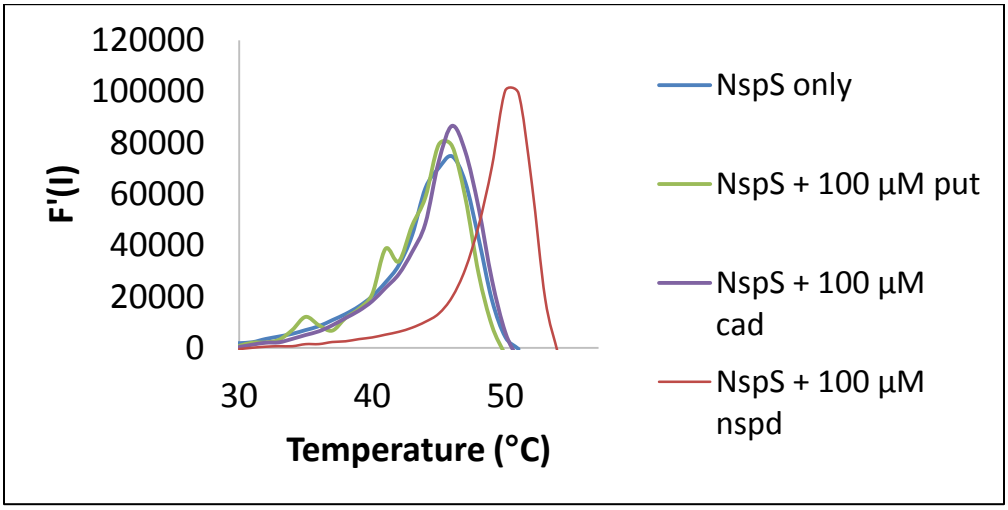

Figure 14: Binding of various polyamines to NspS. Purified NspS protein was combined in 96-well optical plates with SYPRO Orange in reaction buffer only, or increasing concentrations of norspermidine. Blue line-NpsS only, red line-100 µM norspermidine, green line-100 µM putrescine, purple line-100 µM cadaverine. T_m is the peak of respective curves.

The *nspS*$_{E173A}$ mutant produces robust biofilms, expresses *vps* genes at high levels in media only, and is unresponsive to norspermidine and spermidine addition. As such, it was hypothesized that purified NspS mutant protein product would be unable to bind these polyamines. However, TSAs indicate that in the presence of increasing concentrations of norspermidine and spermidine, purified NspS$_{D173A}$ protein increases in thermal stability similarly for both polyamines under the conditions tested (Figure 16). Indeed, a 2°C shift in thermal stability was observed for this protein in the presence of 1 µM norspermidine or spermidine compared to protein alone. Subsequent shifts of 5°C were observed for protein in the presence of 10 µM norspermidine or spermidine, and approximately 8-9°C 100 µM concentrations. These data suggest that, although *nspS*$_{E173A}$ mutants do not respond to either

polyamine with a biofilm phenotype or *vps* transcriptional profile under the conditions tested, purified protein is capable of binding both polyamines *in vitro*.

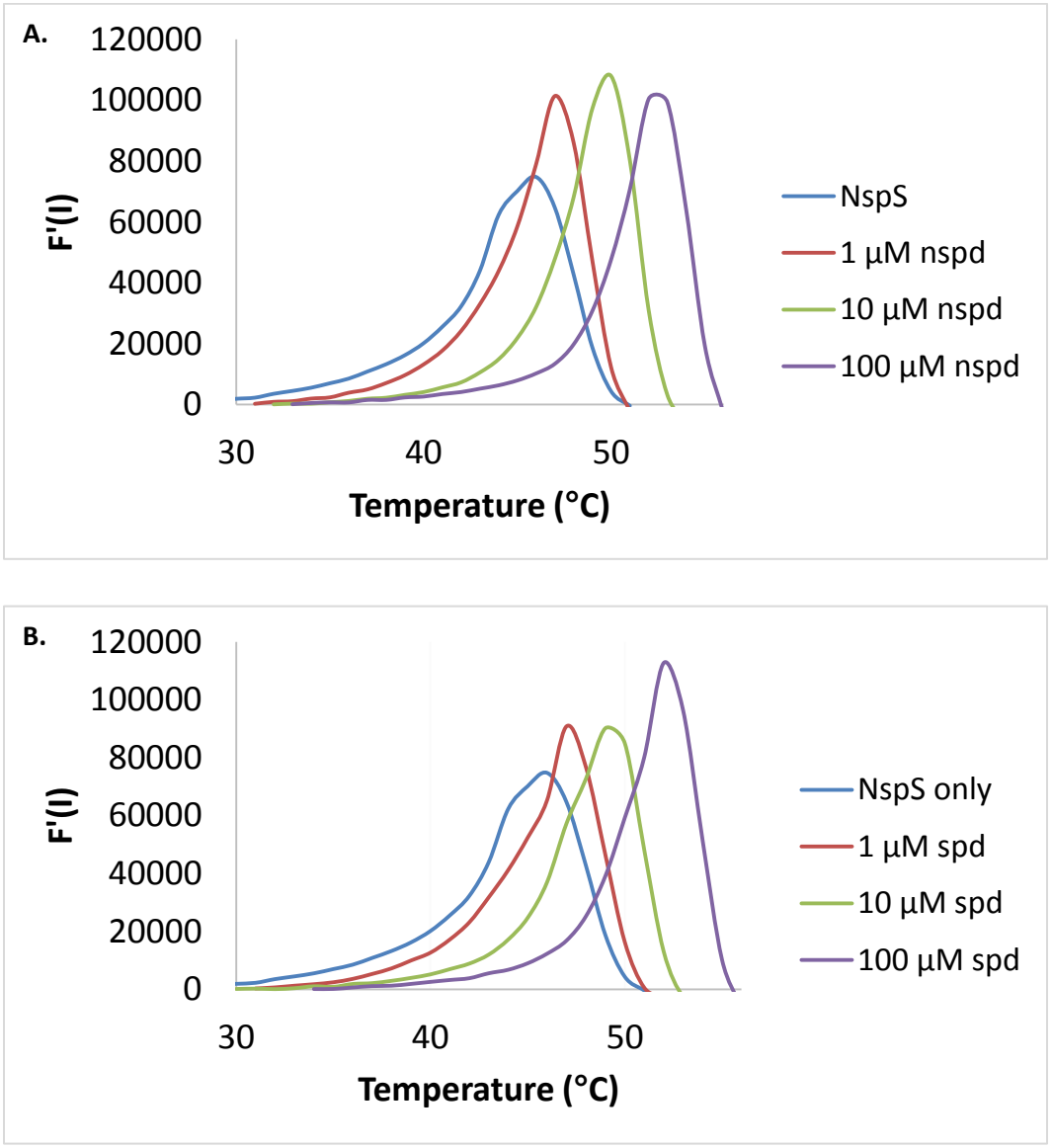

Figure 15: Binding of wild-type NspS to various concentrations of norspermidine (A) and spermidine (B). Blue line-protein only, red line-10 µM polyamine, green line-100 µM polyamine, purple line-1 mM polyamine. T_m is the peak of respective curves.

V. cholerae strains expressing either *nspS*$_{D170A}$ or *nspS*$_{W261A}$ mutants produced low biofilms and *vps* transcripts in the absence of polyamines, yet significantly increased biofilm

formation and *vps* transcription with addition of intermediate and high levels (100 µM and 1 mM) of norspermidine. In contrast, the *nspS*$_{D170A}$ mutant responded to spermidine addition similarly to wild-type when grown in LB medium as both of these strains produced lower levels of biofilms and *vps* transcripts only at 1 mM spermidine. The *nspS*$_{W261A}$ mutant was unresponsive to spermidine. It was therefore hypothesized that NspS$_{D170A}$ may be capable of binding both polyamines, but perhaps to a lesser extent in the case of norspermidine at lower concentrations. Conversely, it was hypothesized that NspS$_{W261A}$ may have a norspermidine-binding profile similar to NspS$_{D170A}$, but a decreased capacity to bind spermidine. However, TSA experiments for both mutants indicate that each protein is capable of binding norspermidine and spermidine at all concentrations tested. In the case of both, NspS$_{D170A}$ and NspS$_{W261A}$, consecutive thermal shifts of 2-3°C, 4-5°C, and 7-8°C are seen for both norspermidine (Figure 17A and 18A, respectively) and spermidine (Figure 17B and 18B respectively). Interestingly, and similar to wild-type NspS protein, norspermidine tends to increase thermal stability by 1-2°C at 1 mM concentrations as compared to spermidine at the same concentration. It is interesting to note that NspS$_{W261A}$ protein unfolding in the absence of polyamines occurred at much lower temperatures than wild-type NspS or other mutants (about 35°C as compared to around 47°C). These observations may indicate that this mutant is less stable than wild-type NspS or the other two mutants under the conditions tested. Additionally, the NspS$_{W261A}$ mutant produced two peaks under all conditions tested indicating that some other variable may be imparting its own effects on the fluorescence curve of this mutant. As the initial stability of this protein appears to be significantly reduced as compare to that of other NspS proteins, it may be possible that a degradation product of the NspS$_{W261A}$ mutant may be forming and that this product maintains the capacity to bind

both polyamines. In this scenario, the fluorescence curve of the derivative product may be imparting its own influences on the curve of the full length protein resulting in the bimodal appearance of these curves under these conditions.

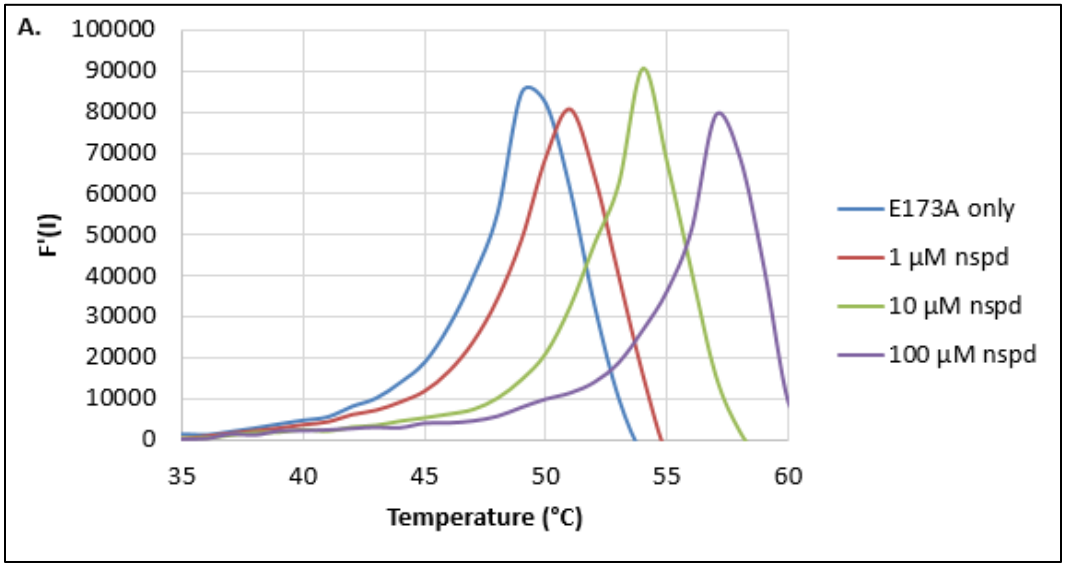

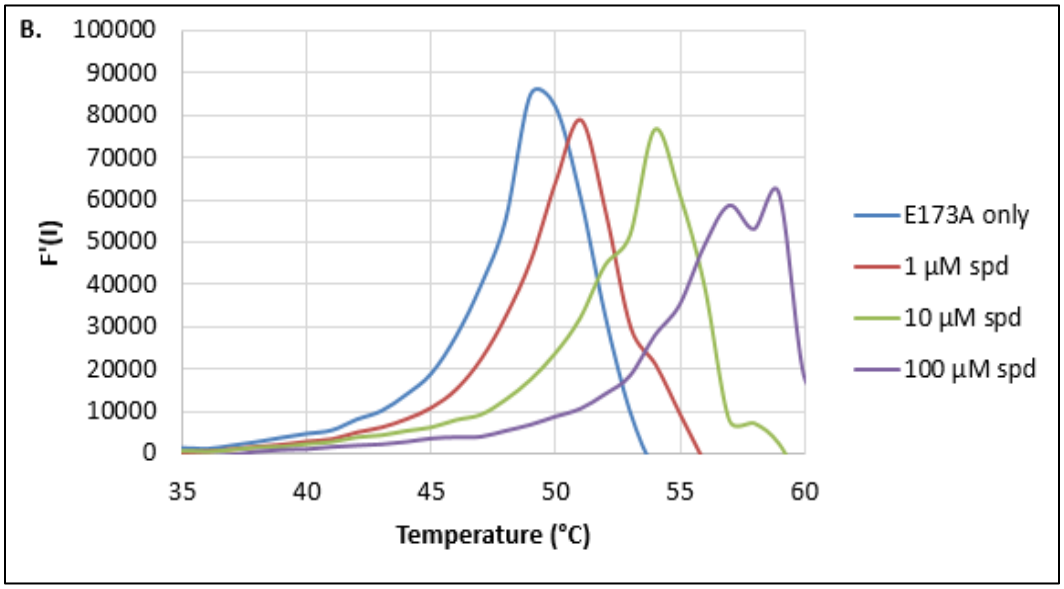

Figure 16: Binding of the E173A mutant to various concentrations of norspermidine (A) and spermidine (B). Blue line-protein only, red line-10 µM polyamine, green line-100 µM polyamine, purple line-1 mM polyamine. T_m is the peak of respective curves.

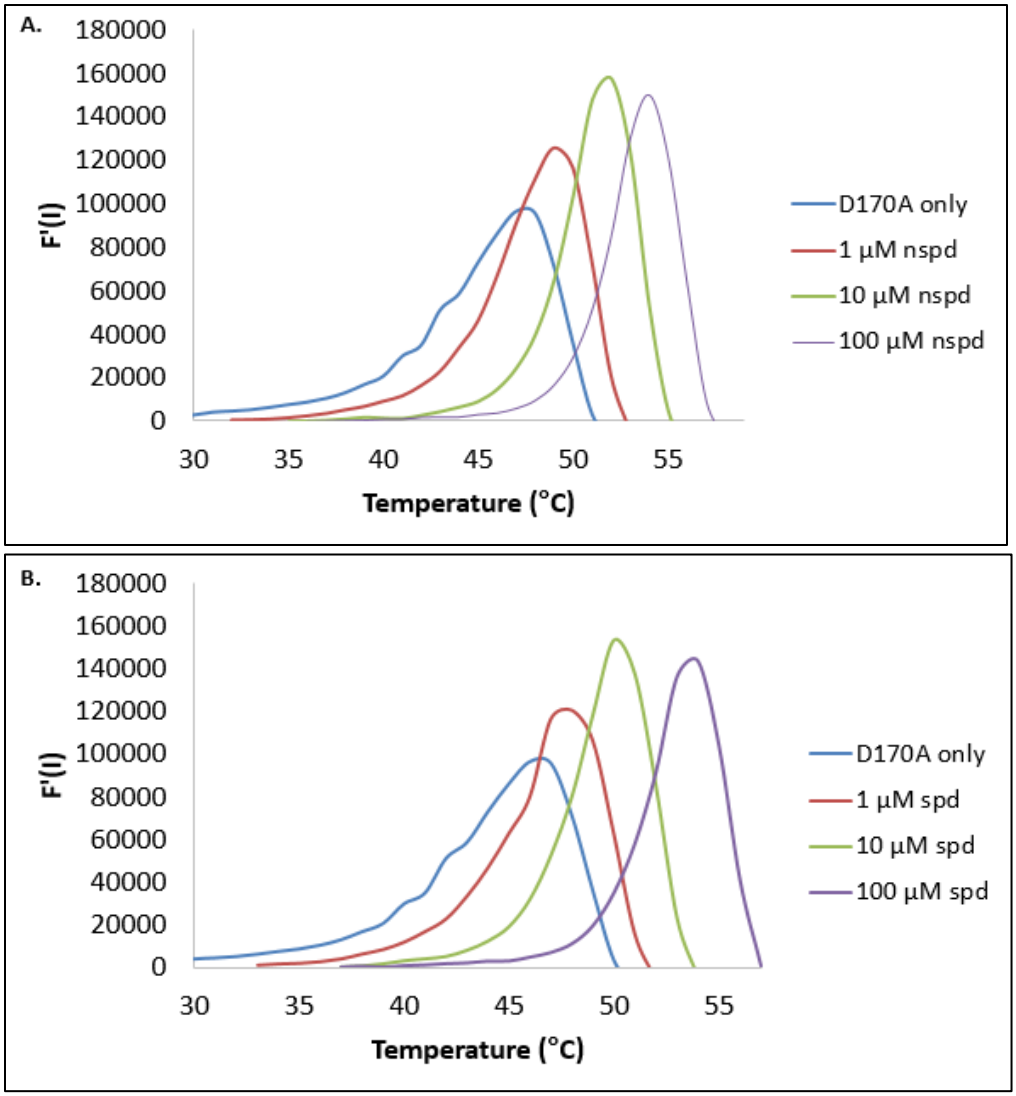

Figure 17: Binding of the D170A mutant to various concentrations of norspermidine (A) and spermidine (B). Blue line-protein only, red line-10 µM polyamine, green line-100 µM polyamine, purple line-1 mM polyamine.

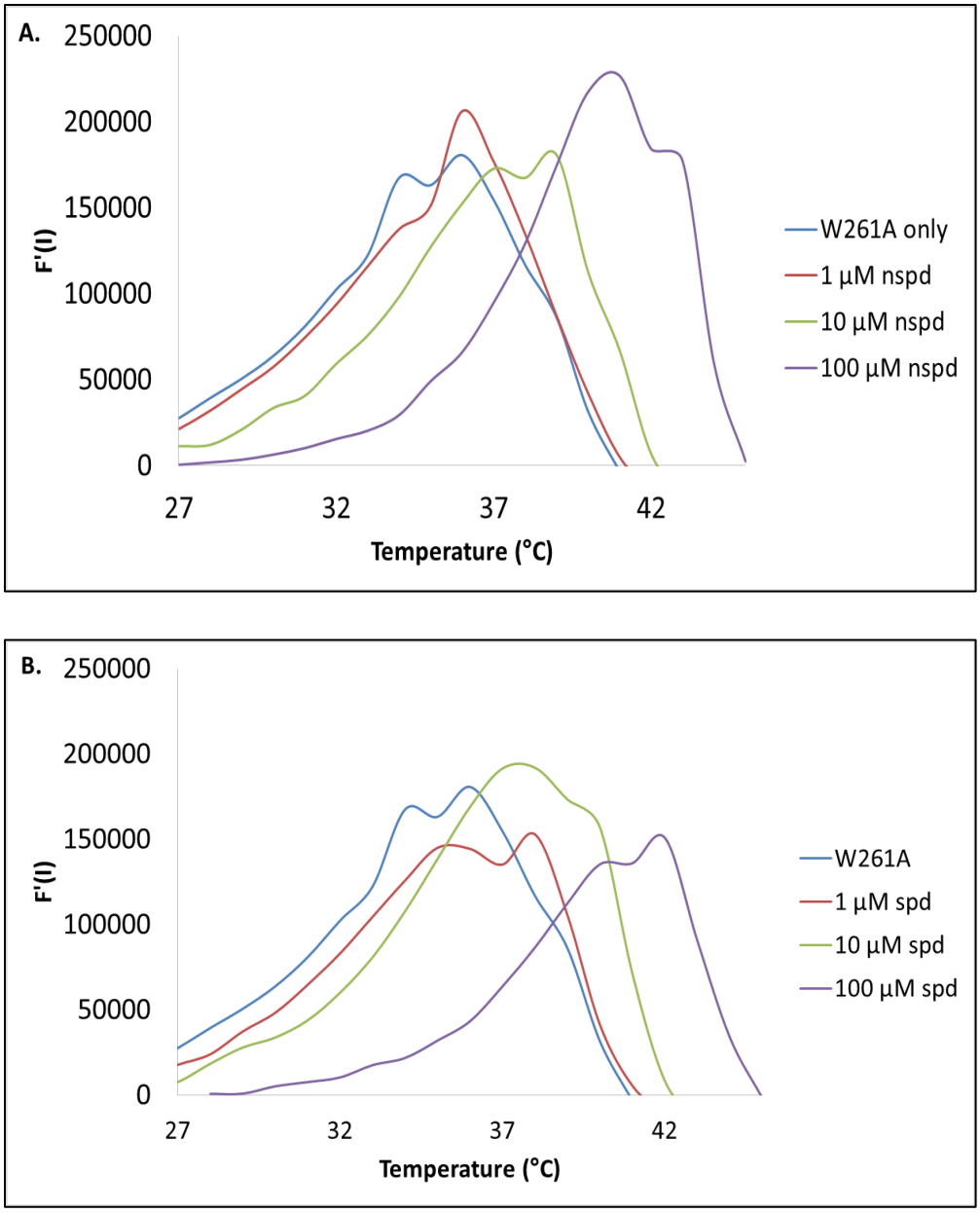

Figure 18: Binding of the W261A mutant to various concentrations of norspermidine (left) and spermidine (right). Blue line-protein only, red line-10 µM polyamine, green line-100 µM polyamine, purple line-1 mM polyamine.

The periplasmic region of MbaA may be expressed in the periplasm independently of the transmembrane and cytoplasmic regions

Generation of pFLMP

Several lines of evidence suggest that NspS and MbaA interact in the periplasm to convey extracellular polyamine signals across the inner membrane to the cytoplasm and control biofilm formation in response to select polyamines. Evidence for the NspS-MbaA interaction has been obtained through co-immunoprecipitation experiments; however, reproducibility has been an issue perhaps due to the low expression of *nspS* and *mbaA* (Brennan WB, Karatan E, unpublished data) in addition to solubility issues with membrane proteins. Therefore, I have developed an alternative approach at studying the NspS-MbaA interaction. To this end, a construct comprising a fusion of the periplasmic region of MbaA, as well as the NspS signal sequence required for periplasmic localization of NspS was developed for expression from an inducible expression plasmid, pFLAG. A flowchart illustrating the cloning strategy employed to generate pFLMP is shown in Figure 19A. Several bioinformatics programs were used to identify the nucleotide sequence encoding the periplasmic domain of MbaA. The 693 base pair nucleotide sequence encoding this domain was amplified by PCR (Figure 19B), gel purified, and spliced at the 5' end to the 99 base pair *nspS* signal sequence with six additional 5' nucleotides encoding two amino acids predicted to be involved in signal peptidase recognition and cleavage to induce periplasmic localization (Figure 19C). The identity and presence of the $mbaA_p$ construct was confirmed by sequencing and colony PCR (Figure 19D), respectively. The approximately 800 base pair construct was ultimately cloned into the pFLAG-CTC expression vector and transformed into a *V. cholerae* Δ*nspS*Δ*mbaA* double mutant with *nspS* complemented on a pACYC184 plasmid.

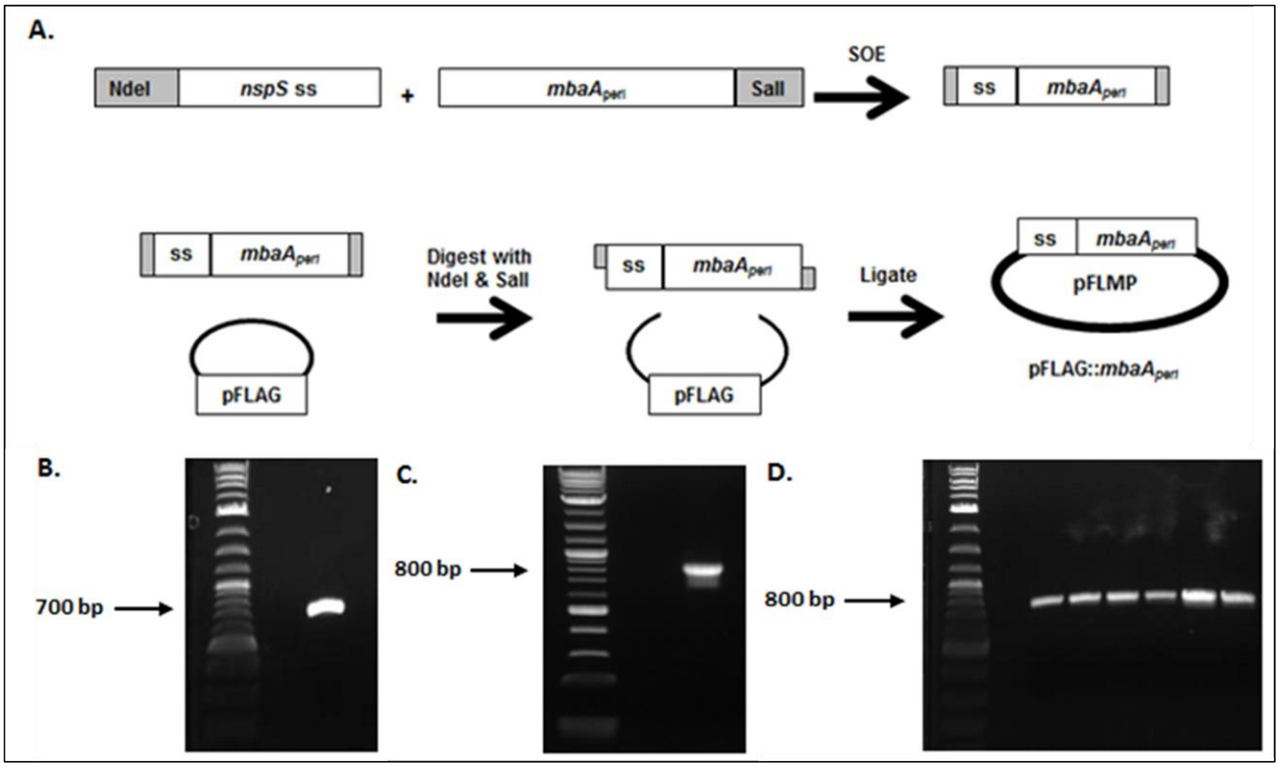

Figure 19: Production of *nspS*$_{ss}$-*mbaA*$_{peri}$ (*mbaA*$_p$). Flowchart of pFLMP construction (A). Gel image of *mbaA*$_{peri}$ PCR product (B). Fusion product of *nspS*$_{ss}$-*mbaA*$_{peri}$ (*mbaA*$_p$) (C). Colony PCR for *mbaA*$_p$ in DH5α candidates with pFLMP (D).

Detection of MbaA$_p$-FLAG and NspS-V5 in the periplasm

Following construction of pFLMP, it was necessary to ensure stability of MbaA$_p$ and confirm periplasmic localization using a Western blot in the presence and absence of NspS. pFLMP was transformed into a Δ*nspS*Δ*mbaA* mutant (PW522) containing the pACYC184::*nspS*-V5 (pNP1) plasmid. Appropriate controls for downstream co-immunoprecipitations were also generated by transforming the double mutant with 1) pNP1 and an empty pFLAG vector to generate AK426 and 2) pFLMP and an empty pACYC184 vector (AK442). Western blots using the anti-FLAG antibody or the anti-V5 antibody were performed with periplasmic extracts from these strains (Figure 20). As seen in the Figure

20A, $MbaA_p$ was detected at 29 kDa in bacteria harboring pFLMP only when grown in the presence of IPTG as expected.

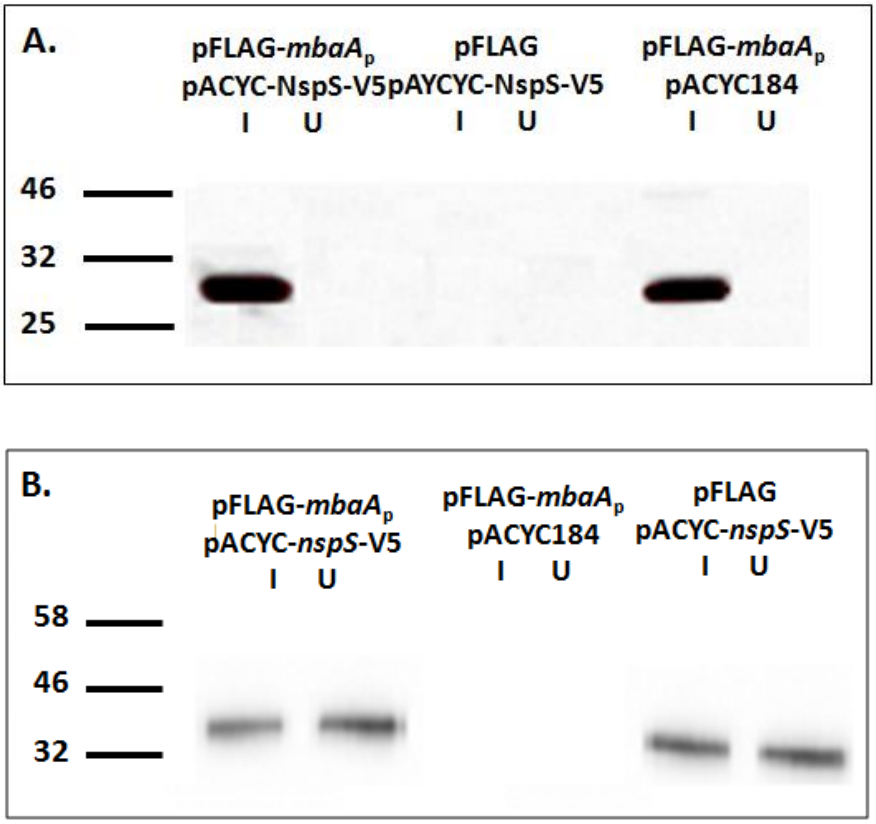

Figure 20: Western blots for $MbaA_p$-FLAG and NspS-V5 expression in the periplasm. Periplasmic fractions were obtained from Δ*nspS*Δ*mbaA* double mutants harboring plasmids encoding NspS-V5 from a pACYC184 vector and/or MbaA-FLAG from a pFLAG vector. For control strains lacking the *nspS*-V5 or *mbaA*$_p$ constructs, the corresponding empty vector was supplied. FLAG antibody (A) and V5 antibody (B). I and U correspond to induced and uninduced culture extracts, respectively.

In contrast, NspS was detected at approximately 40 kDa in all bacteria harboring pNP1 regardless of the growth in the presence (I) or absence (U) of IPTG as predicted for inserts constitutively expressed on the pACYC184 plasmid. (Figure 20B). In strains with pACYC184 or pFLAG plasmids lacking *nspS*-V5 or *mbaA*$_p$ inserts, NspS-V5 or $MbaA_p$ protein was not detected, respectively. Altogether, these data indicate the both NspS-V5 and

$MbaA_p$-FLAG are stable and expressed in the periplasmic fractions of strains harboring the respective pNP1 and pFLMP plasmids.

Co-immunoprecipitation of NspS-V5 and $MbaA_p$

In an effort to show that NspS interacts with the periplasmic region of MbaA, co-immunoprecipitations were performed making use of the inner membrane impermeable crosslinker, BS^3. Mid-log phase cultures were washed and incubated with BS^3 crosslinker with agitation. Periplasmic fractions were extracted and incubated with agarose beads bound to either anti-V5 or anti-FLAG antibodies. Subsequently washed beads (B), periplasmic extracts (E), and unbound fractions (S) of extracts incubated with beads were subjected to Western blots using the reciprocal anti-FLAG (Figure 21A) or anti-V5 antibodies (Figure 21B). As seen in the left panel, $MbaA_p$ was detected in periplasmic extracts and anti-FLAG affinity bead fraction of both strains in which *$mbaA_p$* was expressed regardless of the presence of *nspS*-V5 as indicated by 29 kDa bands. This indicates that nonspecific pull-down of $MbaA_p$ occurred in extracts from strains lacking the *nspS*-V5 complement, potentially due to binding of $MbaA_p$-FLAG to the agarose beads themselves. Similarly, NspS-V5 was detected at approximately 40 kDa in all fractions of strains expressing *nspS*-V5 regardless of presence $MbaA_p$ indicating nonspecific pull-down by anti-V5 agarose beads. Additionally, a wide range of BS^3 concentrations (0, 0.5, 1, 2, 3, and 4, mM) were used in additional experiments to eliminate the possibility of oversaturation with the BS^3 crosslinker which could lead to large oligomers that may be hindered in gel electrophoresis and/or transfer to the PVDF membrane (data not shown). However, while these experiments showed 80 kDa bands indicating potential dimerization of NspS as previously shown [83], the expected band size of 69 kDa comprised of the 29 kDa $MbaA_p$ and 40 kDa NspS-V5 proteins was not

detected. Heterotetramers consisting of NspS and MbaA have been reported in the aforementioned co-immunoprecipitation experiments. Therefore, it is possible that oversaturation of the BS^3 crosslinker is occurring and that NspS-$MbaA_p$ heterotetramers comprising a 138 kDa complex remain undetected in co-immunoprecipitation experiments due to incomplete transfer. Future experiments to investigate this possibility will include performing overnight transfers at 4°C to allow for more complete transfer of larger oligomers. Notably, Figure 21A reveals a 58 kDa band in bead samples of strains expressing *mbaA*$_p$ indicating potential dimerization of $MbaA_p$. Optimization experiments are currently under way to eliminate nonspecific pull-down of target protein in these experiments. Some of these optimization approaches include varying the concentration of BS^3 crosslinker added to resuspended cells and the use of detergents during resin binding steps.

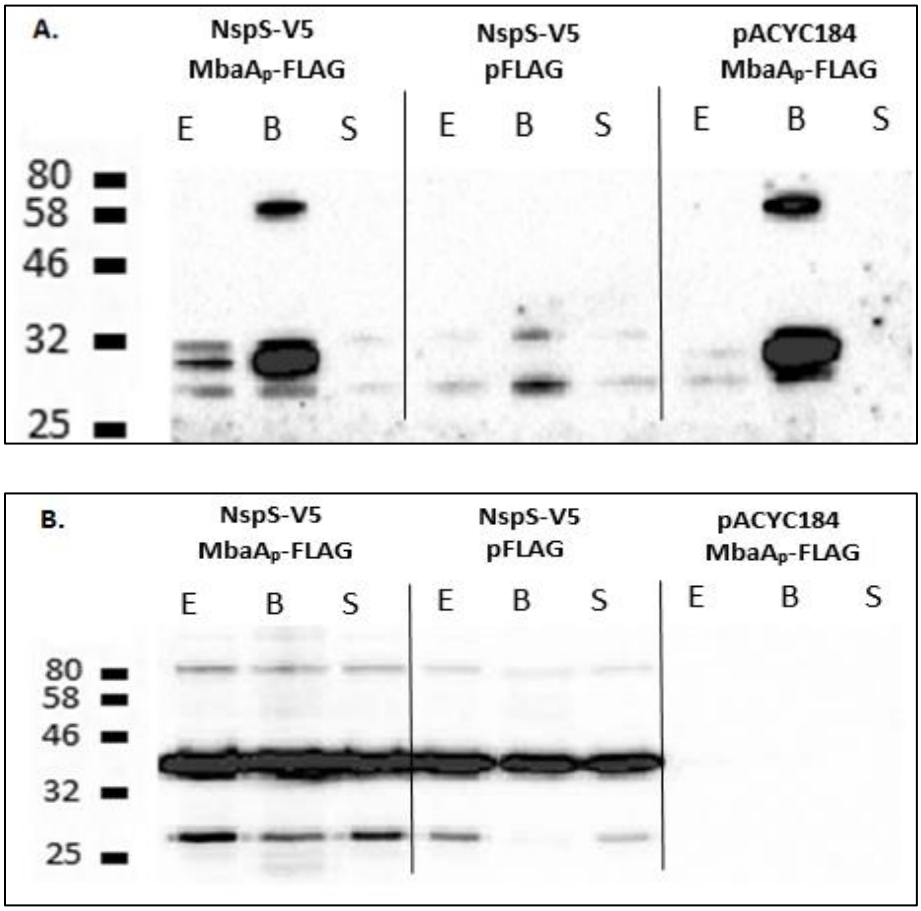

Figure 21: Co-immunoprecipitations for NspS-V5 and $MbaA_p$. A. shows blots with samples pulled down using agarose-anti-V5 beads and subjected to anti-FLAG antibody detection while B. shows blots with samples pulled down using agarose-anti-FLAG beads and subjected to anti-V5 antibody detection. E-periplasmic extracts, B-corresponding agarose beads, S-supernatant from extracts incubated with beads.

Generation and purification of the polyclonal Anti-NspS antibody

Once a reproducible co-immunoprecipitation assay is developed for detection of the proposed NspS-MbaA interaction, the next step will be to identify a binding interface on these proteins. In order to accomplish this, error prone PCR or a mutagenesis kit will be used to generate point mutations along the entirety of the *nspS* sequence and mutants will be cloned into a Δ*nspS* mutant strain of *V. cholerae* to identify NspS mutants defective in

biofilm formation using biofilm assays described above. Using this method, it may be necessary to screen several hundred to several thousand mutants to dismiss those mutations which cause reduced biofilm formation as a result of decreased protein stability, premature stop codons, or mutations at the promoter region. Fast screening approaches such as ELISA would significantly reduce time expenditure and effort required for more tedious approaches such as Western blotting. ELISAs require two antibodies: one specific to the protein of interest to pull down protein from cell extracts, and another specific to a different epitope to be used in detection of the protein in the cell extracts. To this end, a polyclonal anti-NspS antibody could be used as the capture antibody and a second V5 antibody-HRP conjugate which specifically binds the V5 epitope tag fused to the C-terminus of NspS mutants would be used to determine protein levels colorimetrically. Following the initial screening processes, ELISAs could be used to identify strains harboring mutations which inhibit NspS-MbaA binding. In such a scenario, the polyclonal anti-NspS antibody would again serve as the capture antibody. Periplasmic extracts of Δ*nspS*Δ*mbaA* strains harboring the pFLMP plasmid as well as NspS mutants would then be screened for NspS-$MbaA_p$ interaction using the anti-FLAG antibody. For NspS mutants that are unable to interact with $MbaA_p$, colorimetric change would not be observed and corresponding *nspS* mutant genes would subsequently be sequenced to identify the mutations which prevent interaction. Localization of these specific residues could then be determined using homology modeling to map residues likely to be present on the NspS surface. Surface residues which prevent the interaction would likely play a role in mediating said interaction.

In preparation for these screens, a polyclonal anti-NspS antibody was generated against purified NspS protein in rabbits. Previous research in our lab has shown that the

majority of NspS protein produced using the pET28b::*nspS* construct in *E. coli* tends to aggregate in an insoluble form of protein known as inclusion bodies. Recent research has shown, however, that inclusion bodies may be used for antibody generation (Yang et al. 2011). Therefore, urea-based denaturing conditions were used to solubilize NspS inclusions in order to obtain enough NspS antigen for rabbit immunizations and all fractions were analyzed via SDS-PAGE and Coomassie staining as seen in the representative image displayed in Figure 22. Although a large amount of protein remained in the unbound fraction (UBF) and came off in the resin wash (W), a sufficient amount of NspS was recovered in the elution fractions (E1-5) under these conditions. Previously purified NspS protein was used as a secondary size marker (NspS).

NspS inclusions were precipitated following purification via dialysis into PBS, and washed to remove contaminating protein. These inclusions were used in rabbit immunizations over the course of three months prior to sacrifice and harvesting of whole rabbit serum. Antibodies were purified from whole serum using an IgG spin purification kit and compared to the latter using SDS-PAGE and Coomassie staining (Figure 23). As expected for IgG, antibodies purified from whole serum produced a 50 kDa band corresponding to the heavy chain and a very faint 25 kDa band corresponding to the light chain is also present. The purification kit contains a gel resin which binds serum proteins which comprise the majority of what is visible in the whole serum fraction. Following serum protein binding, purified IgG antibody may be collected in the flowthrough.

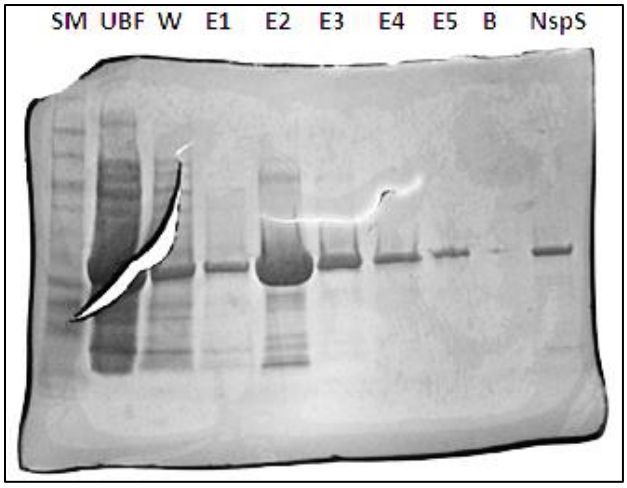

Figure 22: Coomassie-stained SDS-PAGE gel of NspS purified using denaturing conditions. Labels are as follows: SM-size marker, UBF-unbound fraction, W-wash, E1-5-elutions 1-5, B-buffer lane, NspS-purified NspS control.

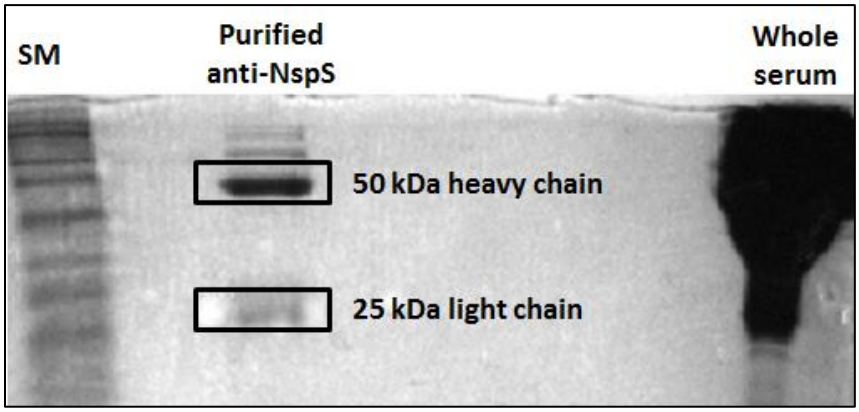

Figure 23: SDS-PAGE gel of purified anti-NspS antibody. Anti-NspS antiobody was purified from whole serum of rabbits immunized with purified NspS inclusion bodies. Boxes surround the 50 kDa heavy chain and the 25 kDa light chain of IgG in the purified antibody lane. Whole serum is present in the far right lane. SM-size marker.

Verification of NspS-specificity by the polyclonal anti-NspS antibody

Purified NspS antibody was then tested for the ability to detect purified NspS protein from various *V. cholerae* periplasmic extracts. Figure 24 shows that periplasmic fractions from strains harboring the native chromosomal copy of *nspS* (357 and 249) produced bands at approximately 40 kDa while strains with the recombinant pACYC184::*nspS*-V5 (AK192)

produced a more prominent band at the same region, each of which ran at the same molecular weight as purified NspS protein suggesting successful anti-NspS antibody generation. In contrast, the 40 kDa band was not detected in a Δ*nspS* mutant.

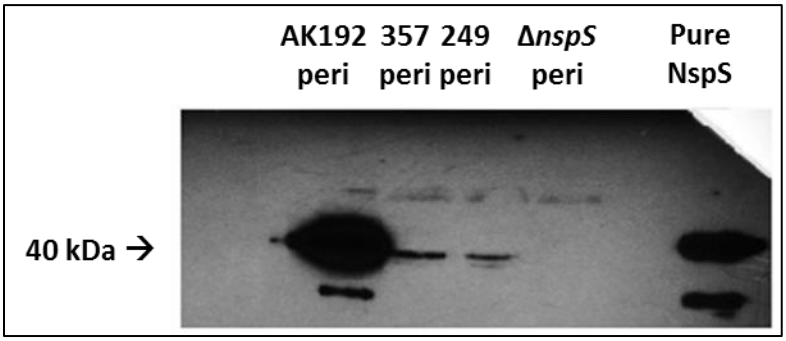

Figure 24: Testing of the polyclonal anti-NspS antibody with periplasmic extracts (peri) and pure NspS. Strains 357 and 249 harbor the native chromosomal copy of *nspS,* AK192 is a Δ*nspS* mutant with the pACYC184::*nspS*-V5 construct, and Δ*nspS* is wild-type *V. cholerae* with a chromosomal *nspS* deletion.

To further test the efficacy of the anti-NspS antibody in the screening procedure described above, ELISAs were performed on various cell fractions obtained by sonication or use of Bugbuster protein extraction reagent. *V. cholerae* Δ*nspS* strains complemented with pACYC184::*nspS*-V5 or vector only were grown to mid-log phase. Anti-NspS antibody was added into wells of high affinity microtiter plates to be used as the capture antibody. Periplasmic extracts or lysates of a Δ*nspS* mutant with vector only or complemented with wild-type *nspS*-V5 were prepared and detected using an anti-V5 antibody-HRP conjugate. As seen in Figure 25, NspS was detected in all preparations from strains harboring NspS-V5. Notably, the periplasmic extract yielded the least amount of nonspecific detection while whole cell lysates prepared by sonication or Bugbuster treatment had comparable levels of nonspecific binding. Color intensity was at least 3.7-fold greater for strains complemented

with wild-type *nspS* regardless of the treatment, indicating a working system for screening against unstable NspS mutants and subsequent interaction experiments.

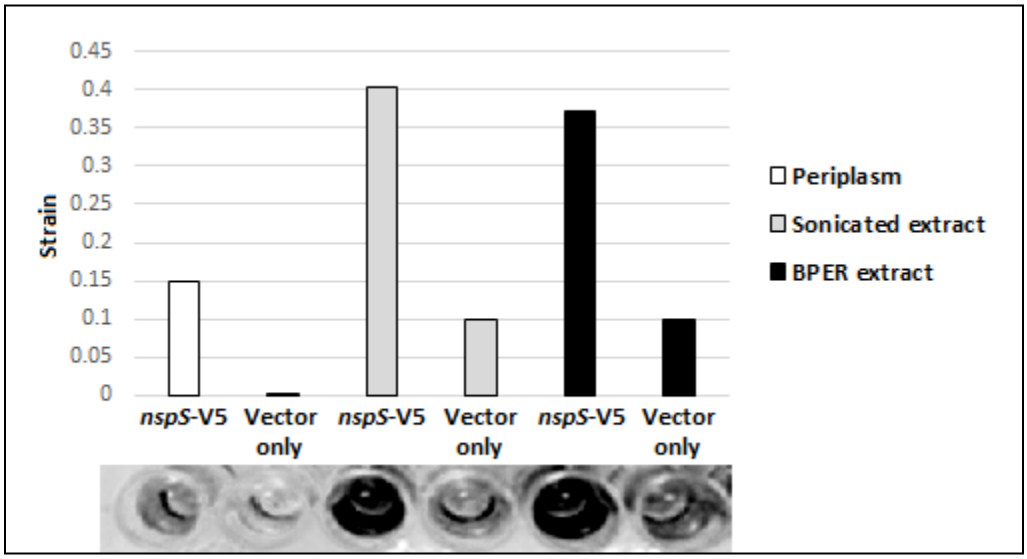

Figure 25: ELISA of wild-type and Δ*nspS* strain extracts. The bar graph (top) shows absorbance intensity at OD_{450} for periplasmic fractions (white bars), or lysates prepared by sonication (grey bars) or bugbuster (black bars) from Δ*nspS* mutants harboring pACYC184 plasmid only (Δ*nspS*) or wild-type *nspS* complement. Wells (bottom) correspond to samples in the bar graph above.

Discussion

The NspS-MbaA pathway has been shown to play a principal role in mediating *V. cholerae* biofilm formation in response to the polyamines, norspermidine and spermidine [47]. This regulation was previously determined to impart such influences on biofilm formation via alterations in *vps* gene transcription through transmission of environmental polyamine signals sensed by NspS to MbaA to modulate c-di-GMP PDE activity of the latter [47]. Additionally, conserved binding pocket residues in NspS had been shown to alter biofilm formation even in the absence of polyamines [82]. However, polyamine responsiveness of these mutants remained to be investigated. Moreover, although MbaA has been shown to have PDE activity *in vitro*, the influences of c-di-GMP levels by this protein in the context of living cells were unknown [81]. Finally, although preliminary data suggests that a direct interaction between NspS and MbaA drives the observed biofilm phenotypes in response to specific polyamines, reproducibility of these experiments has been elusive and the specific NspS residues involved in mediating this interaction have yet to be identified [83]. The main purpose of this study was to thoroughly investigate the mechanisms by which NspS and MbaA control biofilm formation in response to norspermidine and spermidine from polyamine input through to phenotypic output.

While mutation of conserved binding pocket residues in NspS has previously been shown to alter *V. cholerae* biofilm formation, the capacity of these mutants to transmit

polyamine signals had not been investigated. Wild-type *V. cholerae* forms increased biofilms in response to norspermidine at levels as low as 10 µM, and forms even more robust biofilms in the presence of 100 µM norspermidine [47]. In contrast, the inhibitory effect of spermidine on biofilm formation requires levels of around 1 mM. In this study, it was shown that Δ*nspS* deletion complemented with two of three *nspS* ligand-binding pocket mutants, $nspS_{D170A}$ and $nspS_{W261A}$, were mostly desensitized to norspermidine at 10 µM. However, these mutants formed biofilms comparable to a strain complemented with wild-type *nspS* at norspermidine concentrations including 100 µM and 1 mM in both tryptone and LB media, suggesting these residues may influence affinity of NspS to norspermidine. On the contrary, these mutant strains did not respond to spermidine with a biofilm phenotype, indicating that the corresponding aspartate and tryptophan residues may be essential in transmitting spermidine-specific signals. Alternatively, as the biofilms formed by these mutants in the presence of spermidine were similar to that of a Δ*nspS* mutant, these observations may indicate that the influence of MbaA PDE activity is at maximum capacity in the presence of these mutants and can have no further detectable reduction on biofilm formation in response to spermidine. Interestingly, biofilms formed by a Δ*nspS* strain complemented with $nspS_{E173A}$ were comparable to wild-type when grown in tryptone, and significantly more robust when grown in LB. Additionally, this strain did not respond to any concentration of norspermidine tested in this study, indicating that this glutamate residue may be required for dose-dependent responses to this polyamine when grown in either tryptone or LB. Interestingly, while this mutant did not respond significantly to spermidine when grown in LB, biofilms were actually increased when grown in tryptone with 100 µM spermidine and decreased back to levels seen in media alone at 1000 µM spermidine. The increase in biofilm mass at 100 µM levels may

indicate that interactions between spermidine and the Glu173 residue in wild-type NspS could be responsible for distinguishing between norspermidine and spermidine as the latter is a slightly larger molecule and could thus influence the NspS-MbaA interaction surface by pushing against this residue. Therefore, by changing this residue to an alanine, increased free space within the binding cleft may compensate for the addition carbon group of spermidine. However, an increased sample size would be required to increase confidence in these observations particularly considering this observation contrasts with the LB data *vps* transcription results. It is interesting to note that this strain formed biofilms more robust than wild type in LB which is rich in monosaccharides such as glucose, mannose, and galactose, but not in tryptone. This observation may indicate that other players involved in the complex network of environmental signaling and biofilm formation may additionally influence the capacity of NspS and MbaA to modulate this phenotype. That is, perhaps nutrient signals have an additive effect on NspS and/or MbaA signaling potential through cooperative activity of other periplasmic and/or membrane proteins involved in nutrient sensing and transport.

As *V. cholerae* biofilms consist primarily of VPS components, and the effects of norspermidine on biofilm formation have been shown to influence *vps* transcription in a NspS-dependent manner, I hypothesized that the biofilm observations made with *nspS* ligand-binding pocket mutants in response to norspermidine or spermidine should be a direct result of altered *vps* transcription in these mutants. In support of this hypothesis, *vps* activity for Δ*nspS* mutants complemented with $nspS_{D170A}$ or $nspS_{W261A}$ showed reduced *vps* transcription in the absence of polyamines. Furthermore, these mutants showed substantially increased *vps* transcription when grown in the presence of 100 μM norspermidine to levels

comparable to wild-type grown under the same conditions, but did not respond to 1 mM spermidine. Additionally, the *nspS*$_{E173A}$ mutant did not respond to either polyamine, further corroborating the biofilm data.

As alteration of NspS ligand-binding pocket residues have drastic effects on *vps* transcription, biofilm formation, and dose-dependent responsiveness to norspermidine and spermidine, I hypothesized that the corresponding mutants would have a compromised ability to bind these polyamines. Contradictory to this hypothesis, purified NspS ligand-binding pocket mutants underwent thermal shifts comparable to that of wild-type protein in the presence of all norspermidine and spermidine concentrations tested indicating no significant impact on polyamine binding. Notably, the NspS$_{W261A}$ mutant protein alone had a T_m approximately 12°C lower than wild-type indicating that the thermal stability of this mutant is severely altered. Therefore, although *vps* transcription and biofilm phenotypes were eventually observed for strains expressing the *nspS*$_{W261A}$ gene with norspermidine addition, higher concentrations may be required for maintenance of NspS conformational changes which permit signal transduction to MbaA. It has previously been confirmed that all mutants express at the same levels as wild-type; therefore, these observations are not due to decreased protein levels in the cell [82]. Notably, the first derivative of fluorescence curves did not form curves with a single peak, but rather two peaks. This observation may result from contaminating protein detected in protein elutions via SDS-PAGE and Coomassie staining. In future protein purifications, increasing imidazole concentrations in the resin wash may solve the issue of contaminating protein in purified samples.

It is surprising that, although all mutants showed some diminished capacity to transmit norspermidine and spermidine signals, each corresponding purified protein was

capable of binding each polyamine. These observations underline the importance of closely mimicking the physiological conditions during such experiments. It is possible that physiological components of the periplasm may limit or decrease polyamine binding of the mutants *in vivo* such as conformational changes in NspS imparted by interactions with MbaA which alter the topology of the binding pocket. However, it also is possible that, although polyamine binding is permitted by mutants in the periplasm, transmission of the polyamine signal to MbaA is reduced due to alterations in surface topology imparted by such mutations. Indeed the uncharged alanine residue is significantly shorter than aspartate, glutamate, and tryptophan residues, which, with regards to protein scale, may significantly influence signal transmission of signaling proteins. Additionally, the uncharged characteristic differs significantly from that of all three amino acids which would be interacting with polyamines by ionic interactions (e.g., cation-pi interactions in the case of tryptophan) [88]. It could therefore be useful to obtain and compare crystal structures of purified NspS mutants to that of wild-type in the presence of relevant polyamines. Finally, it will be necessary to determine how these mutants interact with and influence the PDE activity of MbaA in response to norspermidine and spermidine. Experiments investigating these aspects of NspS-MbaA signaling are currently under way.

VPS assays corroborate biofilm data and support the hypothesis that modulation of PDE activity of MbaA through interactions with NspS influences c-di-GMP levels in the cell, as increased levels of this second messenger leads to increases in biofilm formation. It is interesting to note that binding pocket residues hypothesized to be involved in polyamine binding have such noticeable effects on biofilm formation even in the absence of polyamines. Also interesting is the observation that although all three NspS mutants tested were able to

bind spermidine and norspermidine, each had unique responses to both polyamines with regards to *vps* transcription and biofilm formation. These findings suggest that while some conserved binding pocket residues are required for both norspermidine and spermidine signaling, others may be essential for signaling extracellular content of one polyamine or the other. Interestingly, although norspermidine is synthesized by *V. cholerae*, norspermidine is not detected in the culture medium, indicating that *V. cholerae* does not export norspermidine; however, many polyamines are acetylated prior to export out of the cell (Sanders, Villa, Karatan unpublished) [89]. Our results indicate that norspermidine may also undergo chemical modifications prior to export and that this modified norspermidine molecule is the more physiologically relevant molecule involved in signaling through NspS. Indeed, *V. cholerae* also contains a homolog of the spermidine N-acetyltransferase from *E. coli*. A recent study screening 95 potential substrates for *V. cholerae* SpeG showed that purified protein interacts with both spermidine and spermine; however, other polyamines, specifically norspermidine, were not included in this screen [90]. Therefore, it remains to be determined whether this protein has evolved to accommodate norspermidine acetylation, and if the acetyl-norspermidine product acts as the true transduction signal in nature.

Polyamine signaling through NspS and MbaA is believed to alter *vps* transcription and biofilm formation through modulation of PDE activity and, in turn, c-di-GMP levels in the cell. Although MbaA is a confirmed c-di-GMP PDE *in vitro*, the impact of cellular c-di-GMP levels through this system had yet to be determined. Using LC-MS/MS analysis of cellular c-di-GMP levels for wild-type *V. cholerae* or a Δ*nspS* mutant grown in media alone or in the presence of norspermidine or spermidine, it was shown that c-di-GMP levels remain at about 45-65 nM, regardless of strain or polyamine addition. This indicates that, although

polyamine addition has significant effects on *vps* transcription and biofilm phenotypes, the contribution of MbaA PDE activity to cellular c-di-GMP levels is insignificant. This observation suggests that the c-di-GMP pool influenced by NspS-MbaA signaling may be subcellularly located. Support for high specificity c-di-GMP signaling has recently been reported [46]. High specificity c-di-GMP signaling is defined as influencing segregated subcellular pools of c-di-GMP to control specific phenotypic outputs. In contrast, low specificity systems would influence global pools of c-di-GMP, and c-di-GMP levels would remain homogenous throughout the entirety of the cell to control these phenotypic responses. Therefore, alterations in biofilm formation would be directly correlated with changes in c-di-GMP concentrations. It appears that, under the conditions tested, polyamine signaling through NspS and MbaA may be subject to high specificity signaling. However, it would be interesting in subsequent experiments to compare c-di-GMP levels of a low biofilm forming mutant (e.g. Δ*nspS*) mutant to that of a robust biofilm former such as the same overexpressing *nspS* to determine if more significant influences on global c-di-GMP levels may be observed under these conditions. This hypothesis is premised on the observation that Δ*nspS* mutants overexpressing wild-type *nspS* exhibited a 4-fold increase in *vps* transcription as compared to the same harboring vector only. As c-di-GMP influences impacts *vps* transcription, it is possible that overexpression of *nspS* from the pACYC184 plasmid could override the fine-tuning of local c-di-GMP signaling through this system allowing more influence of c-di-GMP levels to be observed.

In the current model, NspS-MbaA signal transduction requires a direct interaction between these proteins, and alterations at the binding interface result in conformational changes in MbaA to control PDE activity in response to polyamine binding by NspS.

Therefore, once a reproducible experimental design for showing the NspS-MbaA interaction is developed, it will be necessary to identify specific residues on both proteins which mediate this interaction. However, membrane proteins are notoriously difficult subjects of study due to their insoluble nature in aqueous solution. Therefore, a modified approach employing use of the periplasmic region of MbaA alone was developed to investigate the nature of this interaction. However, under the conditions tested, nonspecific binding of NspS-V5 and $MbaA_p$-FLAG to anti-FLAG or anti-V5 agarose beads occurred in co-immunoprecipitation experiments. These observations are puzzling and may indicate nonspecific binding to pull-down antibody linked to the resin, or binding to the resin itself. Future experiments will be required to optimize interaction experiments. Alternatively, purified NspS protein may be used in ELISA experiments to show the interaction. To this end, the anti-NspS antibody would serve as the capture antibody for purified NspS protein. Next, periplasmic extracts of strains expressing $MbaA_p$-FLAG would be added and detection with anti-FLAG-HRP conjugate would serve to confirm the interaction. However, if nonspecific binding remains an issue, periplasmic extracts could be subjected to size exclusion chromatography to obtain approximately 29 kDa protein and reduce interaction interference by other components of the periplasm and/or nonspecific binding of these other components to NspS.

Following generation of a consistent model system for showing the NspS-MbaA interaction, it will be valuable to delineate the specific residues mediating this interaction in both proteins. One approach for defining these residues on NspS would be to use error prone PCR or a mutagenesis kit to develop a mutant library for the entirety of the NspS amino acid sequence. Mutants would be cloned into an expression vector encoding the V5 epitope tag used throughout this study to which a commercially available antibody may be used in

immunochemistry experiments. Mutants defective in restoring biofilm formation to a Δ*nspS* mutant would be used in a second screen to identify those which are unstably expressed, have mutations within the promoter region thus reducing transcription, or encode premature stop codons would be screened for via ELISA. Using an antibody to the vector-encoded epitope, as well as the polyclonal anti-NspS antibody generated in this study, elimination of these mutants from further screening may be accomplished. A second series of ELISAs may then be used with the same polyclonal anti-NspS antibody as the capture antibody for NspS mutants. Next, periplasmic extracts of strains expressing $mbaA_p$-FLAG would be added and subjected to colorimetric detection using the anti-FLAG-HRP conjugate to identify remaining NspS mutants with hindered interactions with MbaA. Sequencing of the remaining mutants may then be used to map using homology modeling. Finally, inhibition of the interaction may be further confirmed by quantitative chemiluminescent co-immunoprecipitation experiments.

In conclusion, this study provides valuable insights into the mechanisms of NspS-MbaA signaling of environmental polyamines. It was shown that some *nspS* ligand-binding pocket mutants exhibiting diminished *vps* transcription and biofilm formation have reduced sensitivity to norspermidine until higher concentrations are added to culture medium. Additionally, these same mutants are unresponsive to spermidine only, while a third mutant which exhibits increased biofilm phenotypes is unresponsive to norspermidine, but may have acquired to capacity to respond with an increased biofilm phenotype in the presence of 100 μM spermidine. Surprisingly, all three mutants maintain the capacity to bind both polyamines, *in vitro*. Analysis of c-di-GMP levels indicate that polyamine signaling through NspS and MbaA may be a high-specificity system. Finally, several tools for investigating the

final piece of this system, the NspS-MbaA interaction, have been developed including a periplasmic localization system of the periplasmic region of MbaA, and an anti-NspS antibody. Future directions include using these tools in a high through-put immunochemistry-based screening of a NspS mutant library to identify residues involved in mediation of the NspS-MbaA interaction. The plausibility of this approach has been tested through Western blotting and ELISAs. As *nspS*/*mbaA* gene pairs are widely distributed throughout not only *Vibrio* species, but other more distantly related bacteria, determining surface binding patches on these proteins could prove useful for understanding a potentially diverse and novel set of signaling protein pairs [81]. Indeed, it is well documented that signaling proteins are modular, and the interaction interface involved in mediating NspS-MbaA signaling is thus likely employed by other signaling systems aside from that of c-di-GMP modulation [46].

References Cited

1. Beyhan S, Bilecen K, Salama SR, Casper-Lindley C, Yildiz FH (2007) Regulation of rugosity and biofilm formation in *Vibrio cholerae*: comparison of VpsT and VpsR regulons and epistasis analysis of vpsT, vpsR, and hapR. J Bacteriol 189: 388-402.

2. Nielsen PH, Jahn A (1999) Extraction of EPS. Microbial extracellular polymeric substances: Springer p. 49-72.

3. Hung C, Zhou Y, Pinkner JS, Dodson KW, Crowley JR, et al. (2013) *Escherichia coli* biofilms have an organized and complex extracellular matrix structure. MBio 4: e00645-13.

4. Cotter PA, Stibitz S (2007) c-di-GMP-mediated regulation of virulence and biofilm formation. Curr Opin Microbiol 10: 17-23.

5. Karatan E, Watnick P (2009) Signals, regulatory networks, and materials that build and break bacterial biofilms. Microbiol Mol Bio Rev 73: 310-47.

6. Watnick P, Kolter R (2000) Biofilm, city of microbes. J Bacteriol 182: 2675-9.

7. Oliveira NM, Martinez-Garcia E, Xavier J, Durham WM, Kolter R, et al. (2015) Biofilm formation as a response to ecological competition. PLoS Biol 13: e1002191.

8. Chavez-Dozal A, Nishiguchi MK (2011) Variation in biofilm formation among symbiotic and free-living strains of *Vibrio fischeri*. J Basic Microbiol 51: 452-458.

9. Trampuz A, Zimmerli W (2006) Diagnosis and treatment of infections associated with fracture-fixation devices. Injury 37: S59-S66.

10. Battin TJ, Kaplan LA, Newbold JD, Hansen CM (2003) Contributions of microbial biofilms to ecosystem processes in stream mesocosms. Nature 426: 439-42.

11. Paul B, Duthie H, Taylor W (1991) Nutrient cycling by biofilms in running waters of differing nutrient status. J North Am Benthol Soc 10: 31-41.

12. Beloin C, Valle J, Latour-Lambert P, Faure P, Kzreminski M, et al. (2004) Global impact of mature biofilm lifestyle on *Escherichia coli* K-12 gene expression. Mol Microbiol 51: 659-74.

13. Klausen M, Aaes-Jørgensen A, Molin S, Tolker-Nielsen T (2003) Involvement of bacterial migration in the development of complex multicellular structures in *Pseudomonas aeruginosa* biofilms. Mol Microbiol 50: 61-8.

14. Costerton JW, Stewart PS, Greenberg EP (1999) Bacterial biofilms: a common cause of persistent infections. Science 284: 1318-22. PubMed PMID: 10334980.

15. Rice S, Koh K, Queck S, Labbate M, Lam K et al. (2005) Biofilm formation and sloughing in *Serratia marcescens* are controlled by quorum sensing and nutrient cues. J Bacteriol 187: 3477-85.

16. Wai SN, Mizunoe Y, Takade A, Kawabata SI, Yoshida SI (1998) *Vibrio cholerae* O1 strain TSI-4 produces the exopolysaccharide materials that determine colony morphology, stress resistance, and biofilm formation. Appl Environ Microbiol 64: 3648-55.

17. Elasri MO, Miller RV (1999) Study of the response of a biofilm bacterial community to UV radiation. Appl Environ Microbiol 65: 2025-31.

18. Matz C, Kjelleberg S (2005) Off the hook–how bacteria survive protozoan grazing. Trends Microbiol 13: 302-7.

19. Mah T-FC, O'Toole GA (2001) Mechanisms of biofilm resistance to antimicrobial agents. Trends Microbiol 9: 34-9.

20. Vogeleer P, Tremblay YD, Mafu AA, Jacques M, Harel J (2014) Life on the outside: role of biofilms in environmental persistence of Shiga-toxin producing *Escherichia coli*. Frontiers Microbiol 5.

21. Reimer AR, Van Domselaar G, Stroika S, Walker M, Kent H, et al. (2011) Comparative genomics of *Vibrio cholerae* from Haiti, Asia, and Africa. Emerg Infect Dis 17: 2113-21.

22. Kierek K, Watnick PI (2003) Environmental determinants of *Vibrio cholerae* biofilm development. Appl Environ Microbiol 69: 5079-88.

23. Kwan L, Cheung D, Kam K (2003) Peak occurrences of ciguatera fish poisoning precede cholera outbreaks in Hong Kong. Epidemiol Infection 131: 621-6.

24. Faruque SM, Islam MJ, Ahmad QS, Faruque A, Sack DA, et al. (2005) Self-limiting nature of seasonal cholera epidemics: role of host-mediated amplification of phage. Proc Natl Acad Sci U S A 102: 6119-24.

25. Rita R (2009) Cholera and climate: a demonstrated relationship. Trans Am Clin Climatol Assn 120: 119-128.

26. Lucien MAB, Schaad N, Steenland MW, Mintz ED, Emmanuel R, et al. (2015) Identifying the Most Sensitive and Specific Sign and Symptom Combinations for Cholera: Results from an Analysis of Laboratory-Based Surveillance Data from Haiti, 2012–2013. American J Trop Med Hyg 92: 758-64.

27. School YL (2013) Peacekeeping Without Accountability The United Nations' Responsibility for the Haitian Cholera Epidemic. New Haven (CT): Transnational Development Clinic, Jerome N. Frank Legal Services Organization, Yale Law School. Contract No.: October, 30, 2015.

28. Watnick PI, Fullner KJ, Kolter R (1999) A role for the mannose-sensitive hemagglutinin in biofilm formation by *Vibrio cholerae* El Tor. J Bacteriol 181: 3606-9.

29. Islam MS, Drasar BS, Sack RB (1994) The aquatic flora and fauna as reservoirs of *Vibrio cholerae*: a review. J Diar Dis Research 12: 87-96.

30. Huq A, Small EB, West PA, Huq MI, Rahman R, et al. (1983) Ecological relationships between *Vibrio cholerae* and planktonic crustacean copepods. Appl Environ Microbiol 45: 275-83.

31. Ogg JE, Ryder RA, Smith HL (1989) Isolation of *Vibrio cholerae* from aquatic birds in Colorado and Utah. Appl Environ Microbiol 55: 95-9.

32. Waters CM, Lu W, Rabinowitz JD, Bassler BL (2008) Quorum sensing controls biofilm formation in *Vibrio cholerae* through modulation of cyclic di-GMP levels and repression of vpsT. J Bacteriol 190: 2527-36.

33. Morris Jr JG (2011) Cholera—modern pandemic disease of ancient lineage. Emerg Infect Dis 17: 2099-104.

34. Faruque SM, Biswas K, Udden SN, Ahmad QS, Sack DA, et al. (2006) Transmissibility of cholera: in vivo-formed biofilms and their relationship to infectivity and persistence in the environment. Proc Natl Acad Sci U S A 103: 6350-5.

35. Schmid-Hempel P, Frank SA (2007) Pathogenesis, virulence, and infective dose. PLoS Pathogens 3: 1372-3.

36. Huq A, Whitehouse CA, Grim CJ, Alam M, Colwell RR (2008) Biofilms in water, its role and impact in human disease transmission. Curr Opin Biotech 19: 244-7.

37. Hammer BK, Bassler BL (2003) Quorum sensing controls biofilm formation in *Vibrio cholerae*. Mol Microbiol 50: 101-4.

38. Guentzel M, Berry L (1975) Motility as a virulence factor for *Vibrio cholerae*. Inf Immun 11: 890-7.

39. Daniels NA, Shafaie A (2000) A review of pathogenic Vibrio infections for clinicians. Infections Med 17: 665-85.

40. Sondermann H, Shikuma NJ, Yildiz FH (2012) You've come a long way: c-di-GMP signaling. Curr Opin Microbiol 15: 140-6.

41. Hengge R (2009) Principles of c-di-GMP signalling in bacteria. Nat Rev Microbiol 7: 263-73.

42. Cruz DP, Huertas MG, Lozano M, Zárate L, Zambrano MM (2012) Comparative analysis of diguanylate cyclase and phosphodiesterase genes in *Klebsiella pneumoniae*. BMC Microbiol 12: 139.

43. Srivastava D, Harris RC, Waters CM (2011) Integration of cyclic di-GMP and quorum sensing in the control of vpsT and aphA in *Vibrio cholerae*. J Bacteriol 193: 6331-41.

44. Camilli A, Bassler BL (2006) Bacterial small-molecule signaling pathways. Science 311: 1113-6.

45. Dai T, Gupta A, Murray CK, Vrahas MS, Tegos GP, et al. (2012) Blue light for infectious diseases: *Propionibacterium acnes Helicobacter pylori* and beyond? Drug Resist Updates 15: 223-36.

46. Massie JP, Reynolds EL, Koestler BJ, Cong J-P, Agostoni M et al. (2012) Quantification of high-specificity cyclic diguanylate signaling. Proc Natl Acad Sci U S A 109: 12746-51.

47. Karatan E, Duncan TR, Watnick PI (2005) NspS, a predicted polyamine sensor, mediates activation of *Vibrio cholerae* biofilm formation by norspermidine. Journal of bacteriology 187: 7434-43. doi: 10.1128/JB.187.21.7434-7443.2005. PubMed PMID: 16237027; PubMed Central PMCID: PMC1273002.

48. Bomchil N, Watnick P, Kolter R (2003) Identification and characterization of a *Vibrio cholerae* gene, *mbaA*, involved in maintenance of biofilm architecture. J Bacteriol 185: 1384-90. PubMed PMID: 12562809; PubMed Central PMCID: PMC142858.

49. Krukonis ES, DiRita VJ (2003) From motility to virulence: Sensing and responding to environmental signals in *Vibrio cholerae*. Curr Opin Mcrobiol 6: 186-90. PubMed PMID: 12732310.

50. Shikuma NJ, Fong JC, Yildiz FH (2012) Cellular levels and binding of c-di-GMP control subcellular localization and activity of the *Vibrio cholerae* transcriptional regulator VpsT. PLoS Pathogens 8: e1002719.

51. Schaller RA, Ali SK, Klose KE, Kurtz Jr DM (2012) A bacterial hemerythrin domain regulates the activity of a *Vibrio cholerae* diguanylate cyclase. Biochem 51: 8563-70.

52. Hunter JL, Severin GB, Koestler BJ, Waters CM (2014) The *Vibrio cholerae* diguanylate cyclase VCA0965 has an AGDEF active site and synthesizes cyclic di-GMP. BMC Microbiol 14: 22.

53. Tischler AD, Camilli A (2004) Cyclic diguanylate (c-di-GMP) regulates *Vibrio cholerae* biofilm formation. Mol Microbiol 53: 857-69.

54. Römling U, Galperin MY, Gomelsky M (2013) Cyclic di-GMP: the first 25 years of a universal bacterial second messenger. Microbiol Mol Biol Rev 77: 1-52.

55. Ross P, Weinhouse H, Aloni Y, Michaeli D, Weinberger-Ohana P, et al. (1987) Regulation of cellulose synthesis in *Acetobacter xylinum* by cyclic diguanylic acid. Nature 325: 279-281.

56. Paul R, Abel S, Wassmann P, Beck A, Heerklotz H, et al. (2007) Activation of the diguanylate cyclase PleD by phosphorylation-mediated dimerization. J Biol Chem 282: 29170-7.

57. Pei J, Grishin NV (2001) GGDEF domain is homologous to adenylyl cyclase. Proteins: Structure, Function, and Bioinformatics 42: 210-6.

58. Ryjenkov DA, Tarutina M, Moskvin OV, Gomelsky M (2005) Cyclic diguanylate is a ubiquitous signaling molecule in bacteria: insights into biochemistry of the GGDEF protein domain. J Bacteriol 187: 1792-8.

59. Kazmierczak BI, Lebron MB, Murray TS (2006) Analysis of FimX, a phosphodiesterase that governs twitching motility in *Pseudomonas aeruginosa*. Mol Microbiol 60: 1026-43.

60. Schmidt AJ, Ryjenkov DA, Gomelsky M (2005) The ubiquitous protein domain EAL is a cyclic diguanylate-specific phosphodiesterase: enzymatically active and inactive EAL domains. J Bacteriol 187: 4774-81.

61. Tchigvintsev A, Xu X, Singer A, Chang C, Brown G, et al. (2010) Structural insight into the mechanism of c-di-GMP hydrolysis by EAL domain phosphodiesterases. J Mol Biol 402: 524-38.

62. Barends TR, Hartmann E, Griese JJ, Beitlich T, Kirienko NV, et al. (2009) Structure and mechanism of a bacterial light-regulated cyclic nucleotide phosphodiesterase. Nature 459: 1015-8.

63. Ryan RP, Fouhy Y, Lucey JF, Crossman LC, Spiro S, et al. (2006) Cell–cell signaling in *Xanthomonas campestris* involves an HD-GYP domain protein that functions in cyclic di-GMP turnover. Proc Natl Acad Sci U S A 103: 6712-7.

64. Wigren E, Liang ZX, Römling U (2014) Finally! The structural secrets of a HD-GYP phosphodiesterase revealed. Mol Microbiol 91:1-5.

65. Molloy S (2014) Bacterial physiology: HD-GYP domain structure solved. Nat Rev Microbiol 12: 4.

66. Stelitano V, Giardina G, Paiardini A, Castiglione N, Cutruzzolà F, et al. (2013) C-di-GMP hydrolysis by *Pseudomonas aeruginosa* HD-GYP phosphodiesterases: analysis of the reaction mechanism and novel roles for pGpG. PloS 8: e74920.

67. Yildiz FH, Dolganov NA, Schoolnik GK (2001) VpsR, a member of the response regulators of the two-component regulatory systems, is required for expression of vps biosynthesis genes and EPSETr-associated phenotypes in *Vibrio cholerae* O1 El Tor. J Bacteriol 183: 1716-26.

68. Zamorano-Sánchez D, Fong JC, Kilic S, Erill I, Yildiz FH (2015) Identification and characterization of VpsR and VpsT binding sites in *Vibrio cholerae*. J Bacteriol 197: 1221-35.

69. Fong JC, Syed KA, Klose KE, Yildiz FH (2010) Role of Vibrio polysaccharide (vps) genes in VPS production, biofilm formation and *Vibrio cholerae* pathogenesis. Microbiol 156: 2757-69.

70. Yang Q, Defoirdt T (2014) Quorum sensing positively regulates flagellar motility in pathogenic *Vibrio harveyi*. Env Microbiol 17: 960-968.

71. Rutherford ST, van Kessel JC, Shao Y, Bassler BL (2011) AphA and LuxR/HapR reciprocally control quorum sensing in vibrios. Genes Dev 25: 397-408.

72. Srivastava D, Waters CM (2012) A tangled web: regulatory connections between quorum sensing and cyclic di-GMP. J Bacteriol 194: 4485-93.

73. Casper-Lindley C, Yildiz FH (2004) VpsT is a transcriptional regulator required for expression of vps biosynthesis genes and the development of rugose colonial morphology in *Vibrio cholerae* O1 El Tor. J Bacteriol 186: 1574-8.

74. Shikuma NJ, Fong JC, Odell LS, Perchuk BS, Laub MT, et al. (2009) Overexpression of VpsS, a hybrid sensor kinase, enhances biofilm formation in *Vibrio cholerae*. J Bacteriol 191: 5147-58.

75. Tabor CW, Tabor H (1984) Polyamines. Ann Rev Biochem 53: 749-90.

76. Wortham BW, Oliveira MA, Patel CN (2007) Polyamines in bacteria: pleiotropic effects yet specific mechanisms. The Genus Yersinia: Springer p. 106-15.

77. Hamana K, Matsuzaki S (1982) Widespread occurrence of norspermidine and norspermine in eukaryotic algae. J Biochem 91: 1321-8.

78. Parker ZM, Pendergraft SS, Sobieraj J, McGinnis MM, Karatan E (2012) Elevated levels of the norspermidine synthesis enzyme NspC enhance *Vibrio cholerae* biofilm formation without affecting intracellular norspermidine concentrations. FEMS Microbiol Lett 329: 18-27.

79. McGinnis MW, Parker ZM, Walter NE, Rutkovsky AC, Cartaya-Marin C, et al. (2009) Spermidine regulates *Vibrio cholerae* biofilm formation via transport and signaling pathways. FEMS Microbiol Lett 299: 166-74.

80. Karatan E, Duncan TR, Watnick PI (2005) NspS, a predicted polyamine sensor, mediates activation of *Vibrio cholerae* biofilm formation by norspermidine. J Bacteriol 187: 7434-43.

81. Cockerell SR, Rutkovsky AC, Zayner JP, Cooper RE, Porter LR, et al. (2014) *Vibrio cholerae* NspS, a homologue of ABC-type periplasmic solute binding proteins, facilitates transduction of polyamine signals independent of their transport. Microbiol 160: 832-43.

82. Zayner JP (2008) The Regulation of *Vibrio Cholerae* Biofilm by NspS and MbaA. A Thesis: Appalachian State University.

83. Pendergraft SS (2012) Characterization of Protein-Protein Interaction Within a Polyamine Responsive Signaling System in *Vibrio Cholerae*. A Thesis : Appalachian State University.

84. Cockerell SR (2013) A Novel Norspermidine Responsive Signaling Pathway in *Vibrio Cholerae* Affecting Biofilm Formation. A Thesis: Appalachian State University.

85. Giuliani SE, Frank AM, Collart FR (2008) Functional Assignment of Solute-Binding Proteins of ABC Transporters Using a Fluorescence-Based Thermal Shift Assay. Biochem 47: 13974-84.

86. Auclair SM, Bhanu MK, Kendall DA (2012) Signal peptidase I: cleaving the way to mature proteins. Protein Science 21: 13-25.

87. Yang H, Zhang T, Xu K, Lei J, Wang L, et al. (2013) A novel and convenient method to immunize animals: Inclusion bodies from recombinant bacteria as antigen to directly immunize animals. African J Biotech 10: 8146-50.

88. Dougherty DA (1996) Cation-π interactions in chemistry and biology: a new view of benzene, Phe, Tyr, and Trp. Science 271: 163-8.

89. Joshi GS, Spontak JS, Klapper DG, Richardson AR (2011) Arginine catabolic mobile element encoded speG abrogates the unique hypersensitivity of *Staphylococcus aureus* to exogenous polyamines. Mol Microbiol 82: 9-20.

90. Kuhn ML, Majorek KA, Minor W, Anderson WF (2013) Broad-substrate screen as a tool to identify substrates for bacterial Gcn5-related N-acetyltransferases with unknown substrate specificity. Protein Science 22: 222-30.

Vita

Richard Charles Sobe was born in Bradenton, FL. After attending high school at Richlands High School in Richlands, NC, he obtained his Associate in Science degree at Coastal Carolina Community College. He then obtained his Bachelor of Science degree in Biology at Appalachian State University with a concentration in cell and molecular biology and a minor in chemistry. He began working in a research lab under the guidance of Dr. Ece Karatan during his last semester of his undergraduate degree where he remained for the duration of his subsequent graduate school years. After completion of his Master of Science degree in Biology with a concentration cell and molecular biology in 2015, he will determine which PhD program or job opportunity will best foster his professional development as a scientist.